

\*

# CUSPS AND CORES IN GALAXIES: PROBLEMS AND SOLUTIONS

Antonino Del Popolo

Dep. of Physics and Astronomy, Catania University

*October, UFES, Vitoria*

# LECTURE 3:

## Proposed Solutions 2

# Proposed solutions: Summary

- Solutions to the cusp/core problem:
- **Cosmological:**
  - modifying the power spectrum at small scales (e.g. Zentner & Bullock 2003), or
  - modifying the constituent particles of DM (Colin, Avila-Reese & Valenzuela 2000; Sommer-Larsen & Dolgov 2001; Hu, Barkana & Gruzinov 2000; Goodman 2000; Peebles 2000; Kaplinghat, Knox & Turner, 2000)
  - modified gravity theories:  $f(R)$  (Buchdal 1970; Starobinsky 1980),  $f(T)$  (see Ferraro 2012), and MOND (Milgrom 1983a,b)
- **Astrophysical:**
  - are based on the idea that some “heating” mechanism produces an expansion of the DM component of the galaxy, reducing the inner density.
  - Two main categories :**
    - “supernova-driven flattening” (Navarro et al. 1996; Gelato & Sommer-Larsen 1999; Read & Gilmore 2005; Mashchenko et al. 2006, 2008; Governato et al. 2010; Pontzen & Governato 2011),
    - dynamical friction from baryonic clumps (El-Zant et al. 2001, 2004; Romano-Diaz et al. 2008, 2009; Del Popolo 2009; Cole et al. 2011).

# Evidences for Dark Matter

LARGE PART OF THE MATTER IN THE UNIVERSE CONSISTS OF NON-LUMINOUS AND NON-BARYONIC MATERIAL WHOSE ESISTENCE IS INFERRED UNIQUELY THROUGH ITS GRAVITATIONAL INFLUENCE (to date no conclusive evidence of DM (from) relectroweak or other kinds of interactions)

A wide variety of evidence has accumulated in support of dark matter's existence

- **Galaxies**

- Rotation curves

- Gravitational lensing

- Velocity dispersion of stars in some dwarf galaxies ->  $\sim 10^3$  times more mass than can be attributed to their luminosity

- X-ray emission (Ellipticals)

- **Clusters of Galaxy**

- Gravitational lensing

- Velocity distribution and

- Hot gas (X-ray) -> total cosmological matter density of  $\Omega_M \approx 0.2-0.3$

- **Cosmological scales**

- CMB** Anisotropies->  $\Omega_M h^2 = 0.1109 \pm 0.0056$

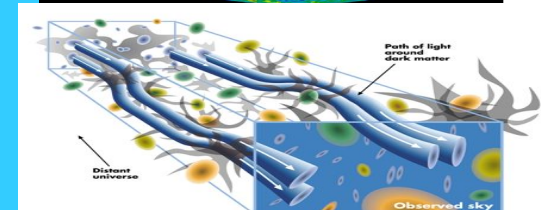
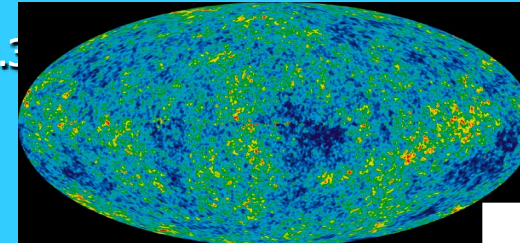
- (improved to  $\Omega_M h^2 = 0.1123 \pm 0.0035$  if distance measurements from BAO and type Ia supernovae are included)  $\Omega_b h^2 = 0.02258$

- (+0.00057, -0.00056) **CMB +BAO+SN**->  $0.02260 \pm 0.00053$

- **Cosmic Shear**

- **Large Scale Structure of the Universe**

- **Structure formation**



# So what is DM?

Big Bang nucleosynthesis (deuterium abundance) and cosmic microwave background (WMAP) determine baryon contribution  $\Omega_B=0.0456\pm0.0016$ ,  $\Omega_M=0.227\pm0.014$  (WMAP+BAO+H $\alpha$ )

**Baryons:** too few to explain all the dark matter because of nucleosynthesis. Moreover unable to drive galaxy formation (decouple too late from photons, not enough time for gravitational instabilities to grow)

$$\frac{\delta\rho}{\rho} \approx A_\lambda \delta \frac{T_m}{T_0} \leq A_\lambda 2 \times 10^{-3}$$

$A_\lambda=1-10$  scale dependent growth factor  $T_m < 0.14$  eV  
 $T_0 = 2.35 \times 10^{-4}$  (CMB temperature now)

$\Omega_{lum} \approx 3 \cdot 10^{-3}$  (stars, gas, dust) (Persic & Salucci (1992); 0.02 (Fukugita, Hogan & Peebles (1998) (including plasmas in groups and clusters)

$\Rightarrow \Omega_B > \Omega_{lum}$

baryonic dark matter has to exist: MACHO, EROS1, etc limits

Rees (1977) : DM could be of a “more

exotic character” -> e.g., small rest mass neutrinos

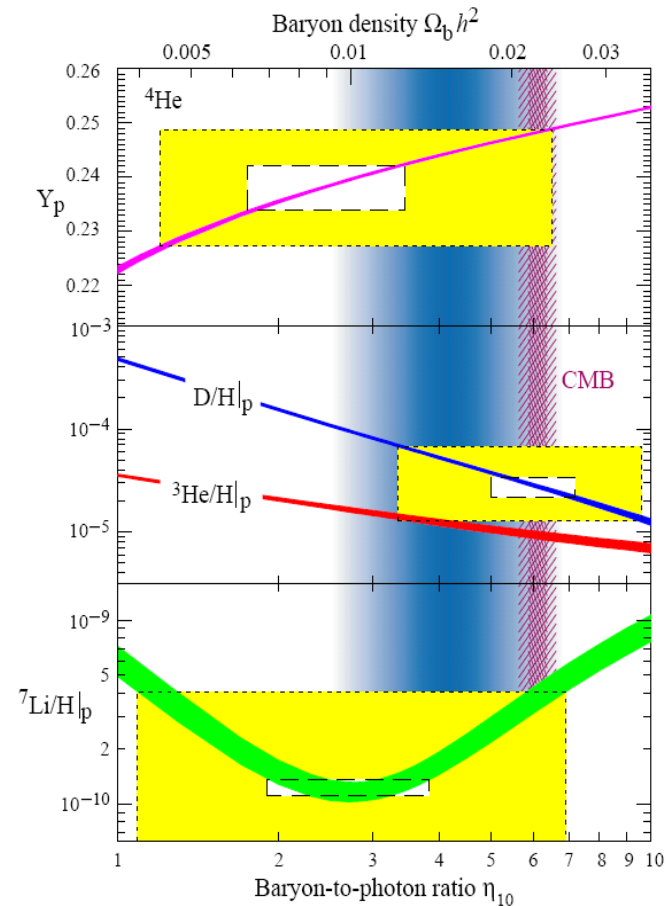
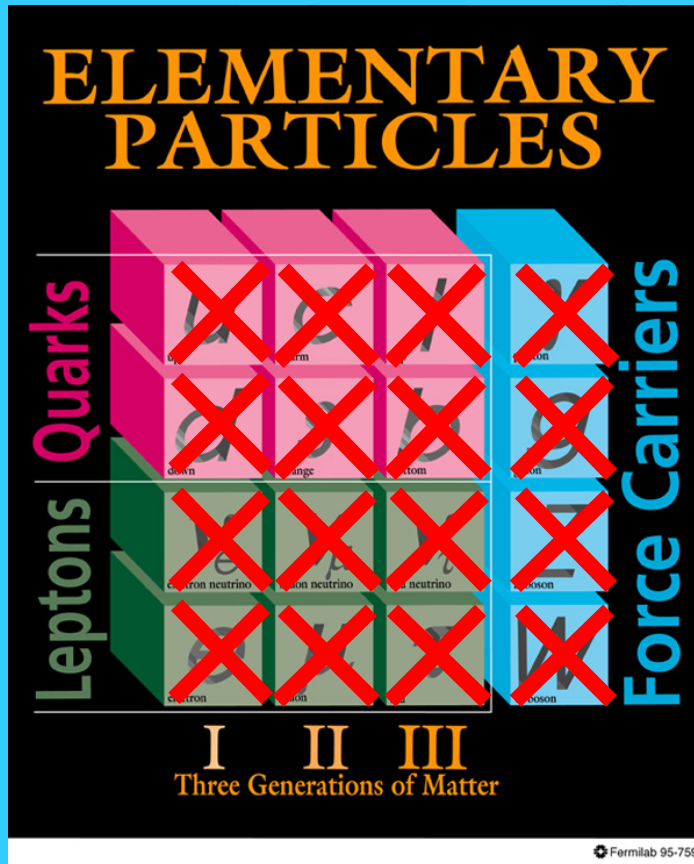


Figure 20.1: The abundances of  $^4\text{He}$ , D,  $^3\text{He}$  and  $^7\text{Li}$  as predicted by the standard model of big-bang nucleosynthesis. Boxes indicate the observed light element abundances (smaller boxes:  $2\sigma$  statistical errors; larger boxes:  $\pm 2\sigma$  statistical and systematic errors added in quadrature). The narrow vertical band indicates the CMB measure of the cosmic baryon density. See full-color version on color pages at end of book.

# The properties of a good Dark Matter candidate:

- **Non-baryonic** (two reasons: BBN, structure formation)
- **Stable** (protected by a conserved quantum number)
- **No charge, No colour** (weakly interacting)
- -if DM non electrically neutral could scatter light -> non DARK
- **cold**, non dissipative (structure formation)
- **relic abundance compatible to observation**

# First place to look for candidates: SM



## Desired DM properties

- Gravitationally interacting
- Not short-lived
- Not hot
- Not baryonic

Unambiguous evidence for new particles

# DARK MATTER candidates

## DM Candidates

### AXION

*Strong CP-problem  
(PQ Symmetry)*

### MSSM LSP

•Hierarchy problem  
  
(bino, wino,  
two neutral  
higgsinos)->Neutralinos;  
3 sneutrinos; gravitino

### UED LKP

*Momentum Conserv.  
(KK-parity):  
KK photon excitation, Z,  
Neutrinos, Higgs bosons  
or graviton*

## “Ad-Hoc” DM Candidates

### keV sterile $\nu$ 's

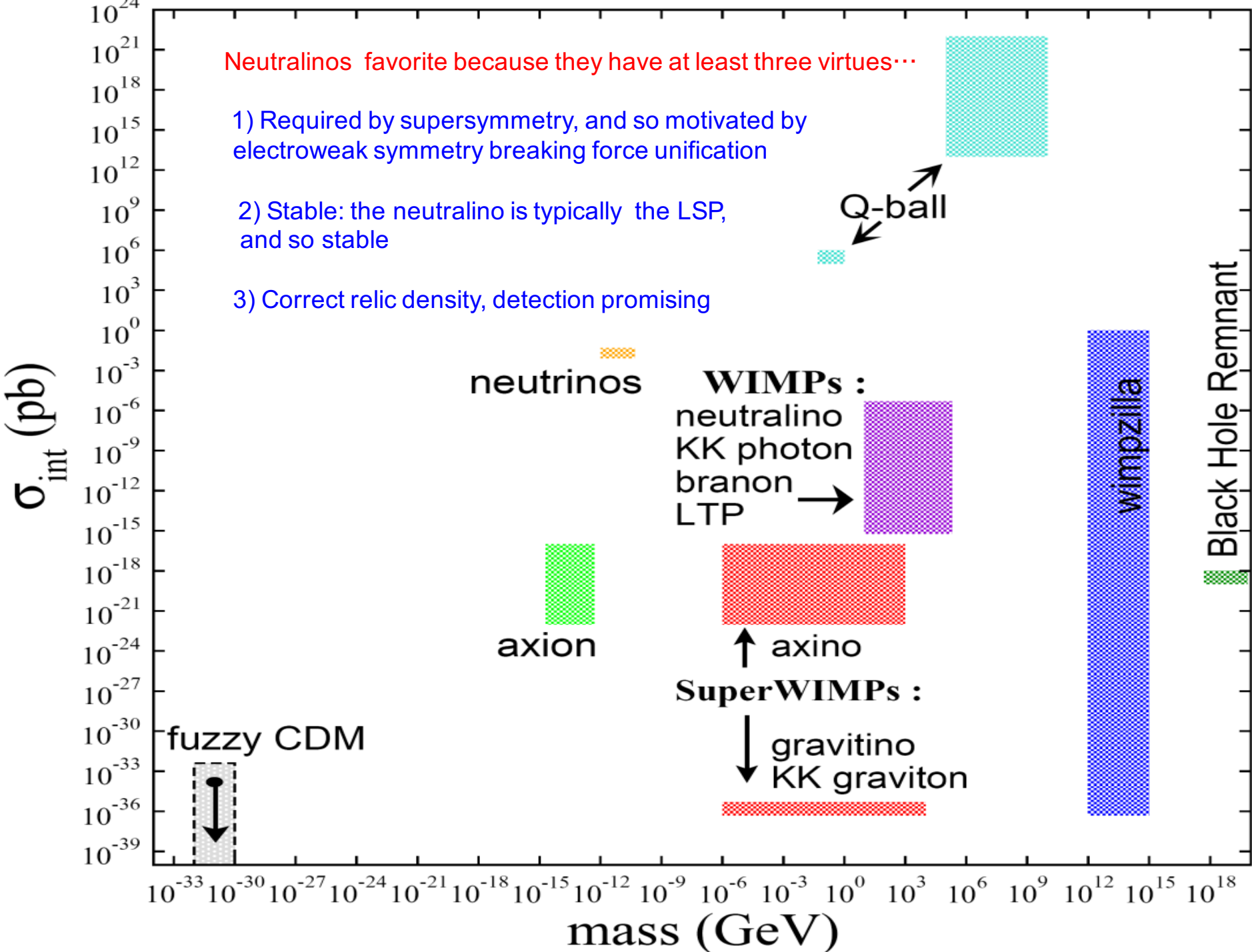
*Neutrino masses  
and mixing  
Warm Dark Matter*

### MeV DM

*511 keV line*

### Super-heavy DM

*Ultra-GZK  
Cosmic Rays  
CR with Energy > Greisen-  
Zatsepin-Kuzmin cut-off*



# DM FORMATION, FREEZE OUT: QUALITATIVE

Assume a new heavy particle  $X$  is initially in thermal equilibrium interacting with the SM particles  $q$ :  $X\bar{X} \leftrightarrow q\bar{q}$  (or  $XX \leftrightarrow q\bar{q}$  if  $X$  is its own antiparticle)

1) In the very early universe when  $T_{\text{Univ}} \gg m_X$  the processes of  $X\bar{X}$  creation and annihilation were equally efficient  $\rightarrow X$  present in large quantities

2) Universe cools:  $T < m_X$  the process of  $X\bar{X}$  creation exponentially suppressed, annihilation process continues.

In thermal equilibrium  $n_{X, \text{eq}} = g_X \left( \frac{m_X T}{2\pi} \right)^{3/2} e^{-m_X/T}$

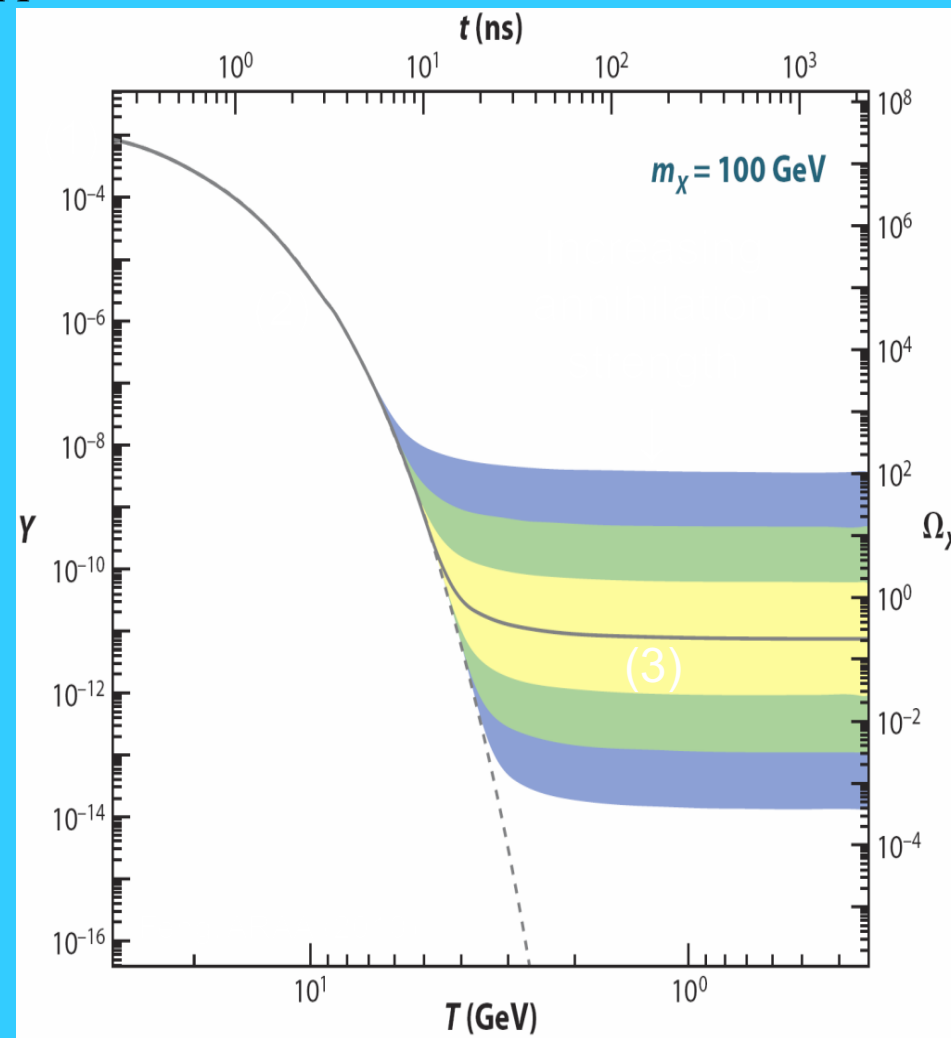


$g_X$  Degree of freedom of  $X$

If particles remain in thermal eq. indefinitely  $\rightarrow$  number density suppressed

3) Self-annihilation contained by the competing Hubble expansion: Universe expands:  $XX \not\rightleftharpoons \bar{q}q$

Expansion  $\rightarrow$  dilution of WIMPs  $\rightarrow$  increasingly dominates over the annihilation Rate  $\rightarrow$  number density of  $X$  sufficiently small that they cease to interact with each other, and thus survive to the present day.



Zeldovich et al. (1960s)

Resulting (relic) density today:

$$\Omega_X h^2 \approx \frac{1.04 \times 10^9 \text{ GeV}^{-1}}{M_{\text{Pl}}} \frac{x_{\text{FO}}}{g_\star^{1/2} (a + 3b/x_{\text{FO}})} \sim x_{\text{FO}} / \langle \sigma v \rangle$$

$$x_{\text{FO}} \equiv \frac{m_X}{T_{\text{FO}}} \approx \ln \left[ c(c+2) \sqrt{\frac{45}{8}} \frac{g_X}{2\pi^3} \frac{m_X M_{\text{Pl}} (a + 6b/x_{\text{FO}})}{g_\star^{1/2} x_{\text{FO}}^{1/2}} \right]$$

$$c \sim 0.5 \quad \langle \sigma_{X\bar{X}} |v| \rangle = a + b \langle v^2 \rangle + \mathcal{O}(v^4)$$

Non-relativistic expansion for heavy states

$g_\star$  number external degrees of freedom = 65, 1 GeV  
 = 120, 1 TeV  
 in SM

If  $X$  has a GeV-TeV scale mass and a roughly weak-scale annihilation cross section, freeze-out occurs at  $x_{\text{FO}} \approx 20 - 30$ , resulting in a relic abundance of

$$\Omega_X h^2 \approx 0.1 \left( \frac{x_{\text{FO}}}{20} \right) \left( \frac{g_\star}{80} \right)^{-1/2} \left( \frac{a + 3b/x_{\text{FO}}}{3 \times 10^{-26} \text{ cm}^3/\text{s}} \right)^{-1}$$

Numerical coincidence? Or an indication that dark matter originates from EW physics?

• For a particle with a GeV-TeV mass, to obtain a thermal abundance equal to the observed dark matter density, we need an annihilation cross section of  $\langle \sigma v \rangle \sim \text{pb}$

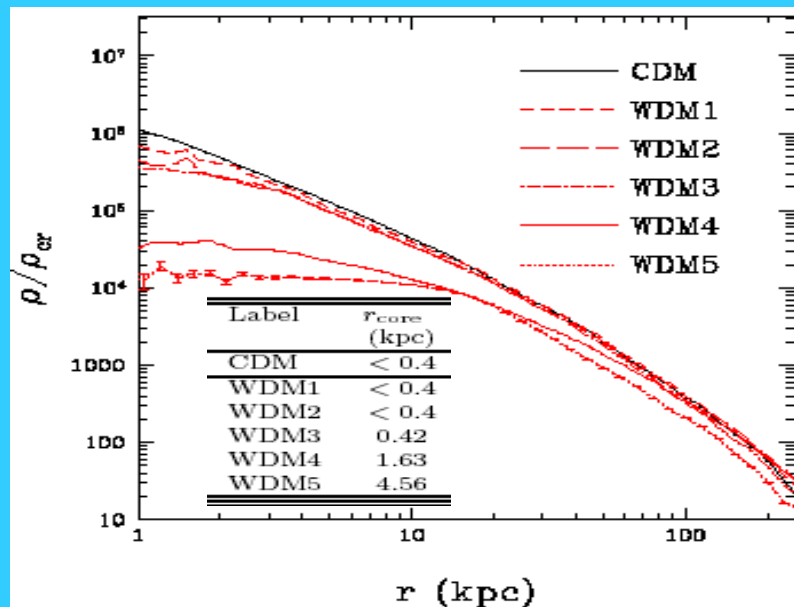
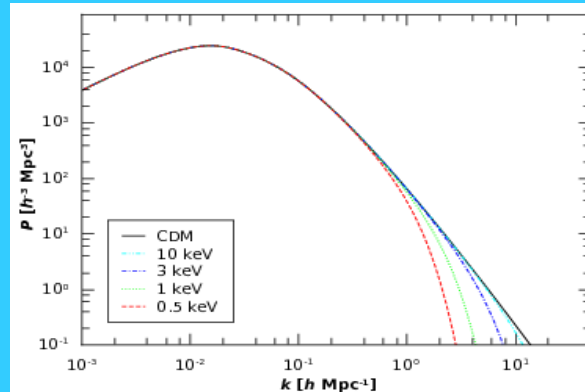
• Generic weak interaction yields:

$$\langle \sigma v \rangle \sim \alpha^2 (100 \text{ GeV})^{-2} \sim \text{pb}$$

WIMP MIRACLE

# Alternatives to (C)CDM

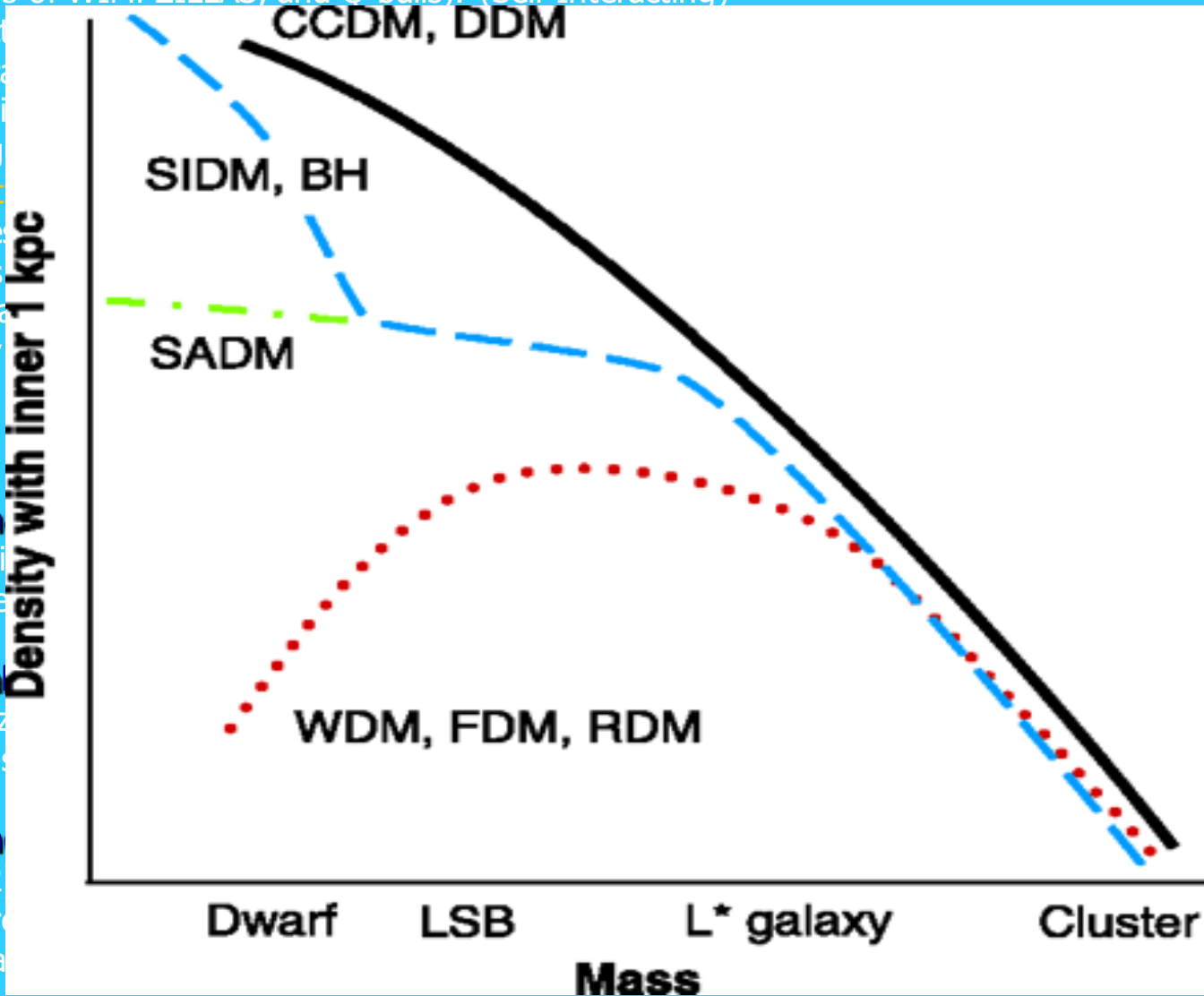
**WDM** (Colin et al. 2000; Sommer-Larsen & Dolgov 2001): (Warm) dispersion velocity (now) 100 m/s; reduce the small scale power, fewer low mass halos, all halos have less steep inner profile. **Problems**, as SIDM (Kuzio de Naray et al. 2010, see SIDM)



A 1 pc core requires a 0.1 keV thermal candidate. Candidates satisfying large scale structure constraints (mv larger than 1-2 keV) the expected size of the core is of the order of 10 (20) pc (Maccio+2012)

**SIDM** (Spergel & Steinhardt 2000; Yoshida et al. 2000; Dave et al. 2001) (Light versions of WIMPZILLAS, and O-balls): (Self-Interacting)

1. Interact
  2. Significa
  3. Scatteri
  - making
  4. Difficult
- high-res  
models  
halo ma  
density



**RDM** (Goodman) particles, similar would behave

**FDM** (Hu et al) size) is the size reduce small-s

**SADM** (Kaplin) (m/GeV) cm<sup>2</sup>  
a. direct re  
b. re-expa

with  
e  
state of DM  
atter halos  
length (effective  
r cores and  
late ( $\sigma \sim 10^{-29}$ )

**DDM** (Cen 2001): (Decaying): if early dense halos decay into relativistic particles and lower mass remnants, then core densities, which form early, are significantly reduced without altering large scale structure

# SIMP

Motivation:

- SIDM may have QCD interaction but not EM
- Not detectable in WIMP search, blocked.

$$8 \times 10^{-25} < \frac{\sigma/\text{cm}^2}{m/\text{GeV}} < 10^{-23}.$$

CMB & LSS constraint:

Before decoupling, photons and baryons are tightly coupled, interaction with baryon will cause additional damping of perturbation

# Modified Gravity (MG)

## MOND

- In 1983, Milgrom proposed a modified Newtonian dynamics in which  $F=ma$  is modified to  $F=ma\mu$ , which  $\mu$  is 1 for large acceleration, becomes  $a/a_0$  when  $a$  is small.

$$F = \frac{GMm}{r^2} = ma\mu,$$

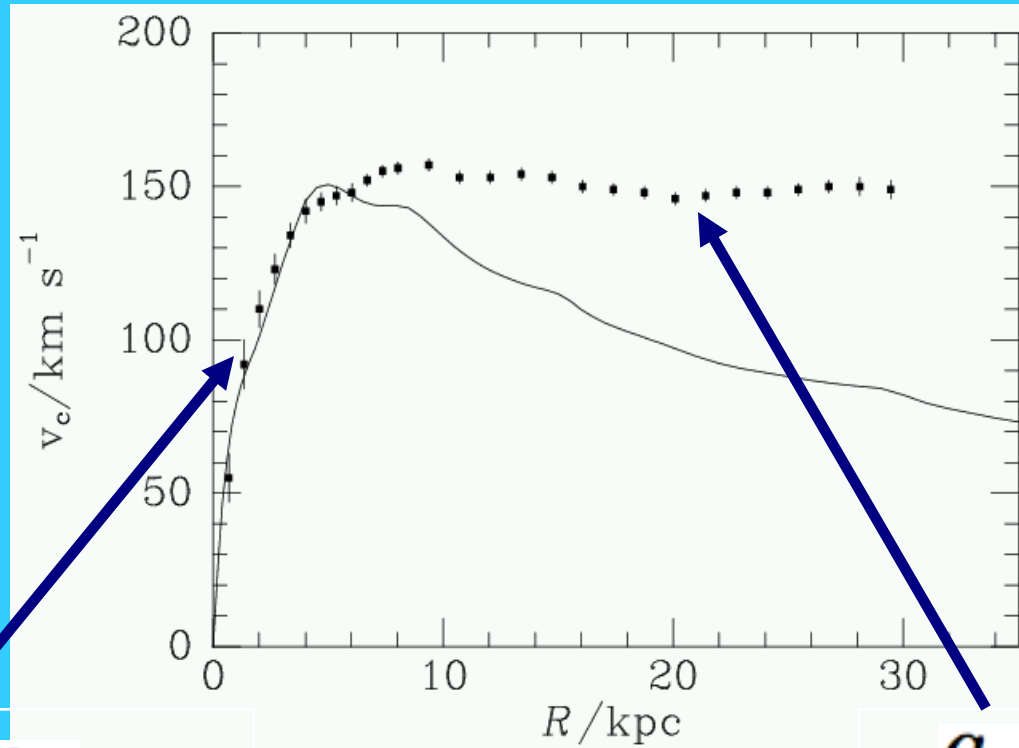
$$a = \frac{\sqrt{GMa_0}}{r}.$$

- To explain the rotational curve, one can choose

$$\frac{\sqrt{GMa_0}}{r} = \frac{v^2}{r} \implies v = (GMa_0)^{1/4}.$$

$$a_0 \sim 1.2 \times 10^{-10} \text{ m/s}^2.$$

MOND



Milgrom, 83

$$a \gg a_0$$

$$a \propto \frac{GM}{R^2}$$

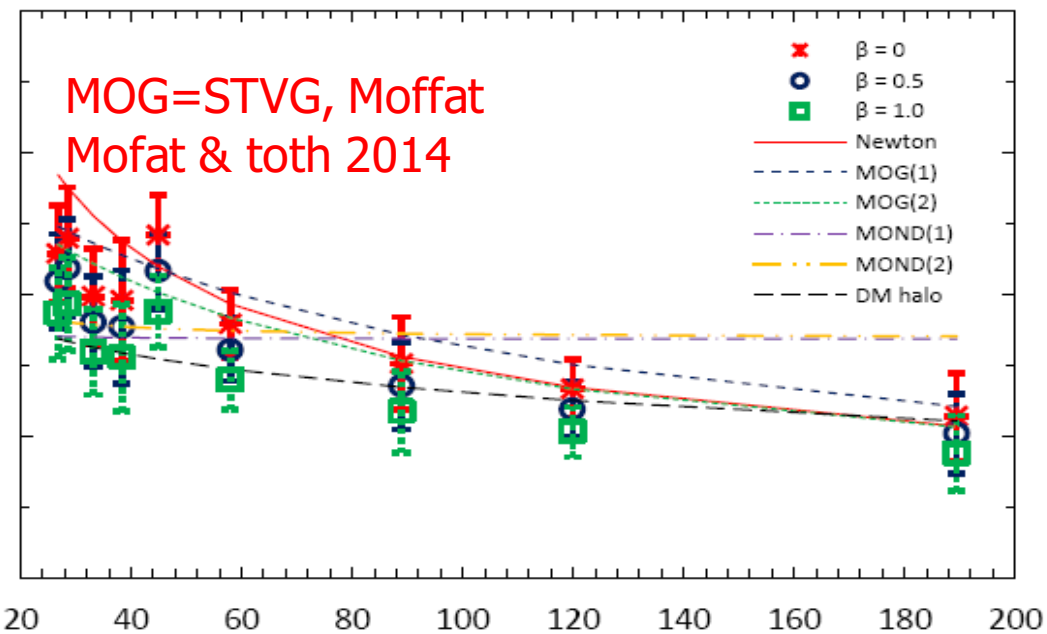
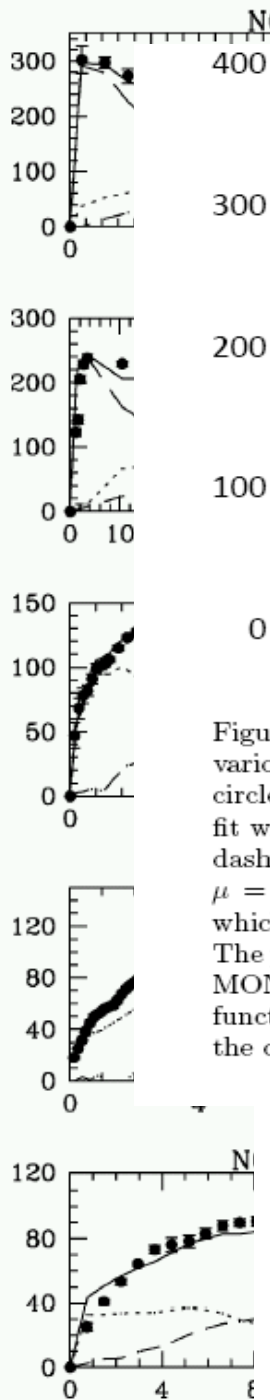
Newton OK

$$a_0 \sim 10^{-8} \text{ cm/s}^2$$

$$a \ll a_0$$

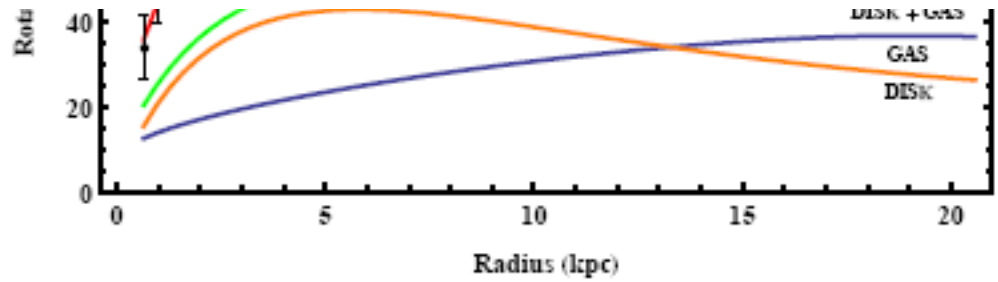
$$a^2 \propto \frac{GM}{R^2}$$

$$v^2 \rightarrow \text{Constant}$$



MOG=STVG, Moffat  
Mofat & toth 2014

Figure 1: Fits to the observed rotational velocities of the Milky Way galaxy using various theories. The data [6] are represented with red crosses ( $\beta = 0$ ), blue hollow circles ( $\beta = 0.5$ ) and green hollow squares ( $\beta = 1.0$ ). The solid red line is the Newtonian fit with a central mass of  $M = 5 \times 10^{11} M_{\odot}$ . The blue medium dashed and green short dashed lines correspond to MOG using the values of  $M = 4 \times 10^{10} M_{\odot}$ ,  $\alpha = 15.01$ ,  $\mu = 0.0313 \text{ kpc}^{-1}$ , and  $M = 5 \times 10^{10} M_{\odot}$ ,  $\alpha = 8.89$ ,  $\mu = 0.04 \text{ kpc}^{-1}$ , respectively, which correspond to the values calculated according to Ref. [7], or given by Ref. [3]. The purple dash-dotted line and the yellow dash-double-dot line correspond to fits using MOND, the mass of  $M = 5 \times 10^{10} M_{\odot}$ ,  $a_0 = 1.21 \times 10^{-8} \text{ cm/s}^2$ , and the interpolation functions given by Eqs. (6) and (7), respectively. Finally, the black long-dashed line is the dark matter halo prediction given in [13].



with the  
ne  $a_0$

Sanders et al

- Iocco, Pato, Bertone (2015):  $a_0$  for MW different from that of other galaxies
- Adams+2015: dwarfs,  $a_0$  non constant
- Randriamampandry, and Carignan (2014): 15 dwarfs and spirals:  $a_0$  different than that postulated by MOND, bad fits.
- Similar results: Boyarsky+2009;..... Cardone & Del Popolo 2012; Saburova & Del Popolo 2015;

# Problems with MOND

- Cannot fit into a framework consistent with GR.
- Hard to describe the expansion history, therefore the CMB fluctuation and galaxy distribution.
- Hard to explain the bullet cluster.
- No MOND can explain all gravitational anomalies without introducing DM.
- MOND violates isotropy of space, linearity, covariance and may not be used to fit any data
- Structure formation => presence of some dark matter component even for models with modified gravity

**OTHER MGs: How to get a MG theory**

# Newtonian Gravity -> GR

$$\vec{a} = -\vec{\nabla}\Phi$$

$$\nabla^2\Phi = 4\pi G\rho_B$$

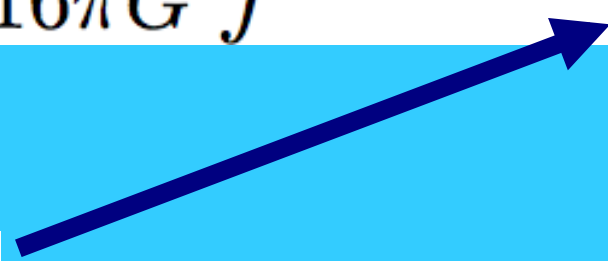
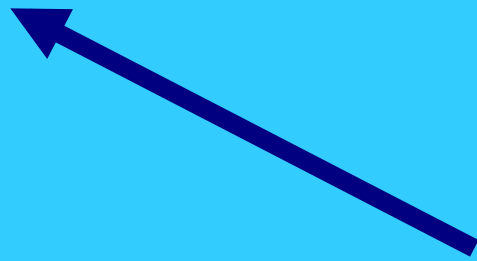


Geodesic

Einstein-Hilbert

$$a^\mu + \Gamma^\mu_{\alpha\beta}v^\alpha v^\beta = 0$$

$$\frac{1}{16\pi G} \int d^4x \sqrt{-g} R(g)$$



$$g_{\alpha\beta}$$

Spacetime metric

# Simplest approach: modify the Einstein-Hilbert action

$$\frac{1}{16\pi G} \int d^4x \sqrt{-g} \mathcal{F}(R, R_{\alpha\beta}, R_{\alpha\beta\mu\nu}, \dots)$$

- Sakharov (1967)- quantum corrections of the Einstein-Hilbert action; low energy string theory
- Higher derivatives of the metric.
- Need it to change at low curvature
- **New degrees of freedom (frozen modes become dynamical)- new fields.**

- 1998: Universe acceleration

⇒ Thousands of work in **Modified Gravity**

( $f(R)$ , Gauss-Bonnet, Lovelock, non-minimal scalar coupling,  
non-minimal derivative coupling, Galileons, Hordenski etc)

[Copeland, Sami, Tsujikawa Int.J.Mod.Phys.D15], [Nojiri, Odintsov Int.J.Geom.Meth.Mod.Phys. 4]

- Almost all in the **curvature-based** formulation of gravity

# Keep Einstein Hilbert action

Geodesic

$$a^\mu + \Gamma_{\alpha\beta}^\mu v^\alpha v^\beta = 0$$

Gravity

$$\frac{1}{16\pi G} \int d^4x \sqrt{-g} R(g)$$

$$g_{\mu\nu}$$

Common metric

# Keep Einstein Hilbert action

Geodesic

$$a^\mu + \Gamma^\mu_{\alpha\beta} v^\alpha v^\beta = 0$$

Gravity

$$\frac{1}{16\pi G} \int d^4x \sqrt{-g} R(g)$$

~~$g_{\mu\nu}$~~

Different metrics

# "Bimetric" theories

Use two different metrics

"Physical" in  
Geodesic equations



"Geometric" metric  
in Einstein equations



$$g_{\mu\nu} = e^{-2\phi} \tilde{g}_{\mu\nu}$$

Dirac, Jordan, Brans, Dicke

**Again! New degrees of freedom (new fields)**

# "Bimetric" theories

Use two different metrics

"Physical" in  
Geodesic equations

"Geometric" metric  
in Einstein equations


$$g_{\mu\nu} = e^{-2\phi} (\tilde{g}_{\mu\nu} + A_\mu A_\nu) - e^{2\phi} A_\mu A_\nu$$

Bekenstein, 04

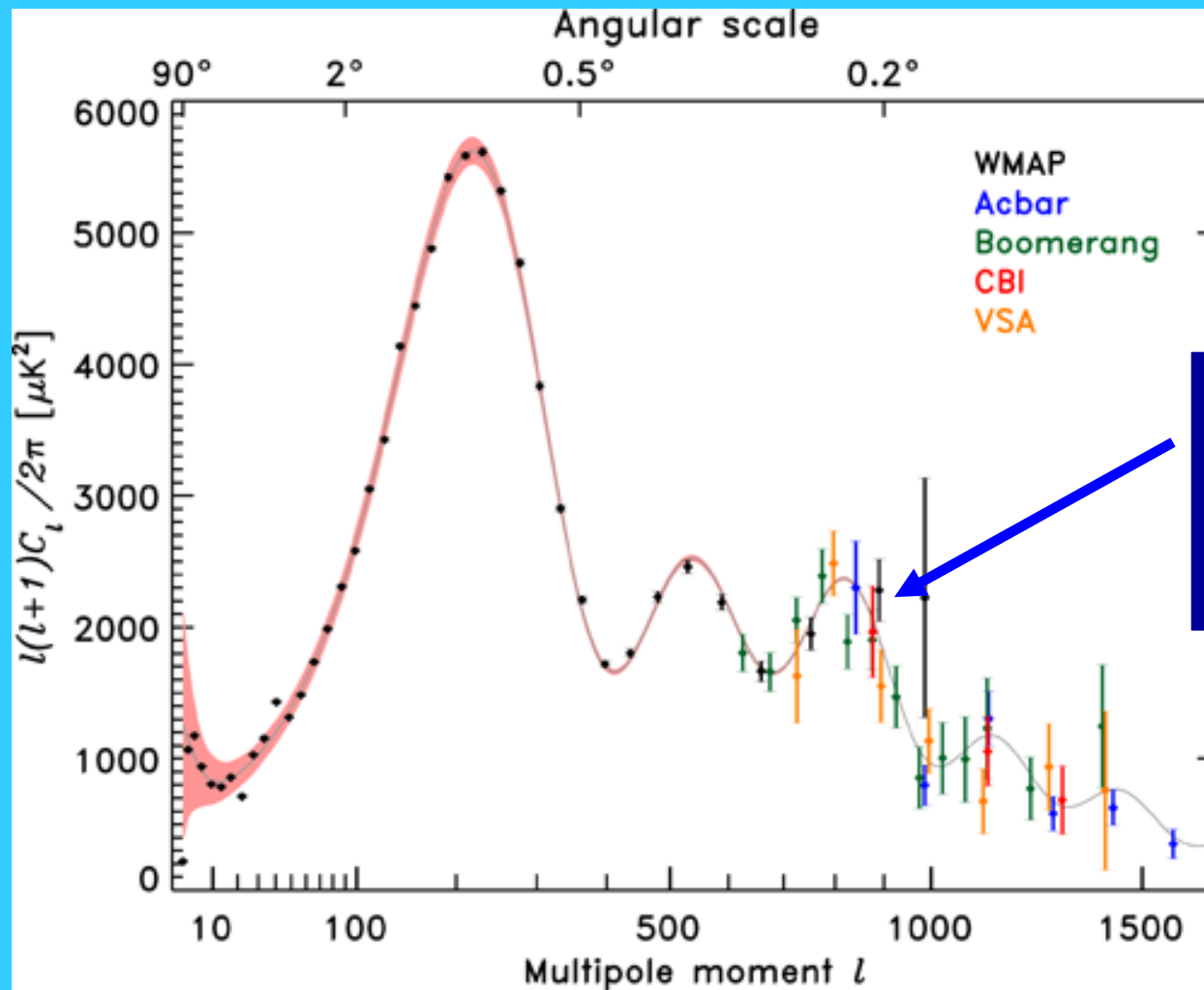
$$\tilde{g}_{\alpha\beta} A^\alpha A^\beta = -1 \quad \leftarrow \text{Time-like ("aether")}$$

**Again! New degrees of freedom (new fields)**

# Extra degrees of freedom ...

Is modified gravity simply a  
more contrived form of  
Dark Matter?

# The Cosmic Microwave Background



3rd Peak is sensitive to dark matter

Remember: extra degrees of freedom drive gravity

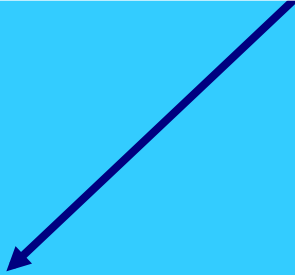
$$\nabla^2 \Phi = 4\pi G \delta \rho_B + \mathcal{S}_1(\alpha, \Phi, \Psi)$$

Pushes up peaks



but ...

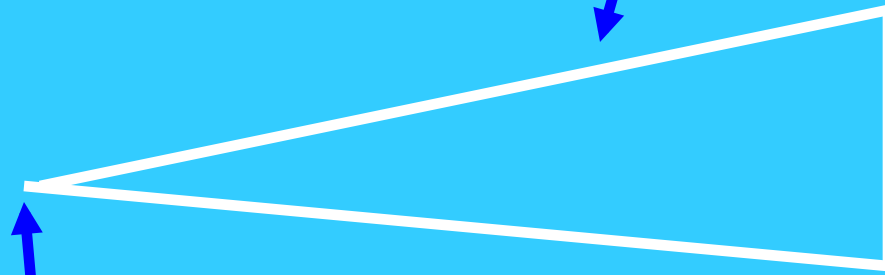
Boosts large scales as well



$$\nabla^2 (\Phi - \Psi) = \mathcal{S}_2(\alpha, \Phi, \Psi)$$

The position of the peak

Distance to surface  
of last scatter

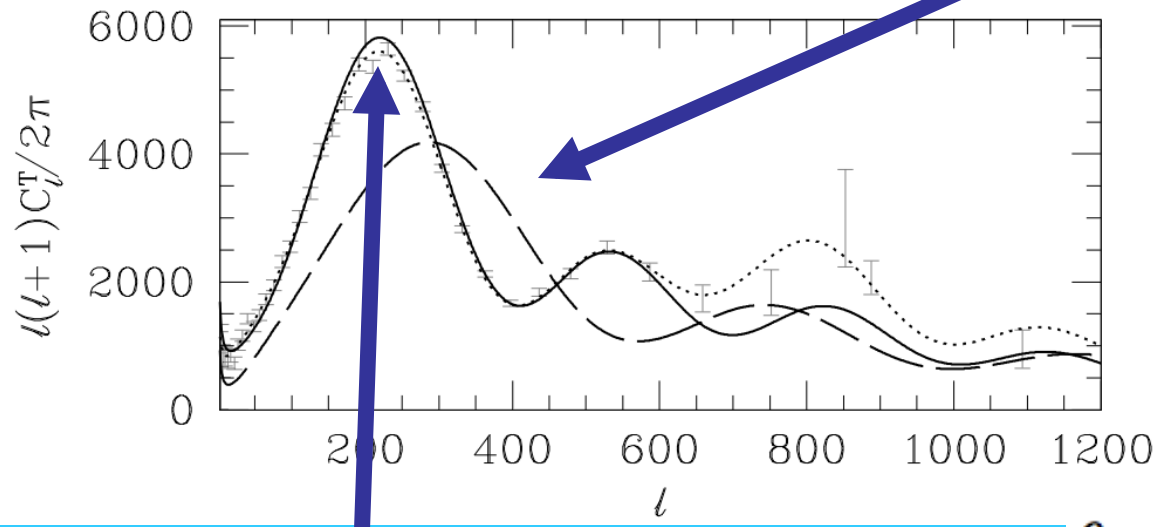


Size of sound horizon  
at last scatter

Position of CMB peak

Position of CMB peak is very well constrained:

$$\Omega_{\Lambda} = 0.95 \quad \Omega_B = 0.05$$



Need  $m_{\nu} = 2.2 \text{ eV}$   
to fit peaks ...

$$\theta = \frac{D_{ls}}{D_0[\Omega_B, \Omega_{\Lambda}, \dots]}$$

... not generically true (Ferreira et al)

- There are now a range of relativistic theories:
  - All have some problems
  - **All have extra degrees of freedom (just like dark matter)**
- Tests should be chosen wisely to disentangle extra degrees of freedom, modified gravity and non-"Birkoffianess"

# Is there a smoking gun for modified gravity?

Analogy with PPN approach:

One may find the non-relativistic limit of GR by considering perturbations about Minkowski space-time in the *conformal Newtonian gauge*

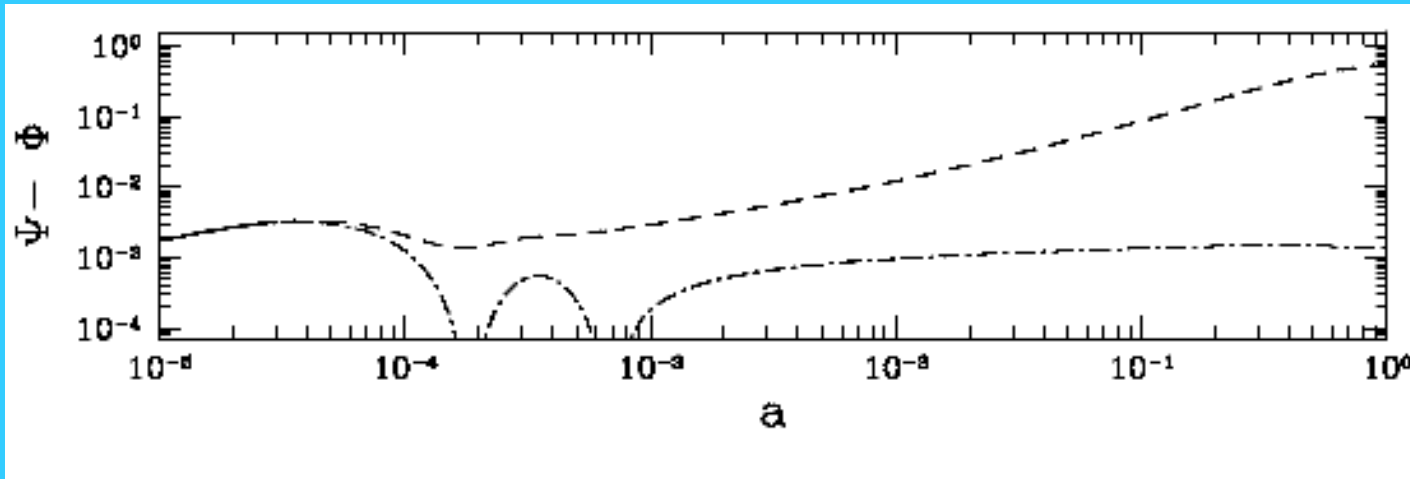
$$ds^2 = -\left(1 - \frac{2GM}{r}\right)dt^2 + \left(1 - \frac{2\gamma GM}{r}\right)dr^2 + r^2 d\Omega^2$$

$$\Phi \neq \Psi$$

$\gamma$  : deviations from Einstein

$$|1 - \gamma| \sim \begin{cases} 10^{-4} & \text{Solar System} \\ 10^{-2} & \text{Galaxies} \\ 10^{-1} & \text{Clusters} \end{cases}$$

$\Phi - \Psi \neq 0$  on cosmological scales



TeVS

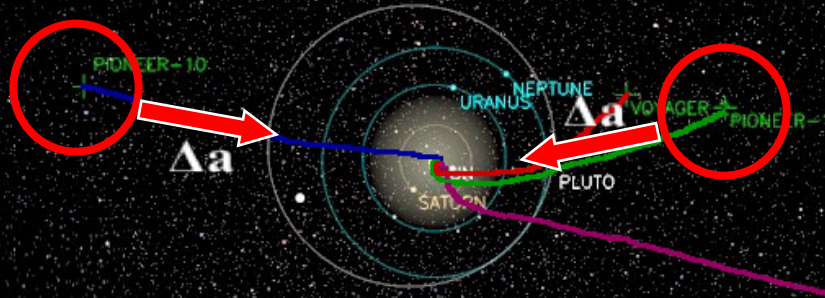
Liguori et al

And changes the growth of structure

# Tests on the scale of Solar system

View of Solar System from above  
2007 APR 04

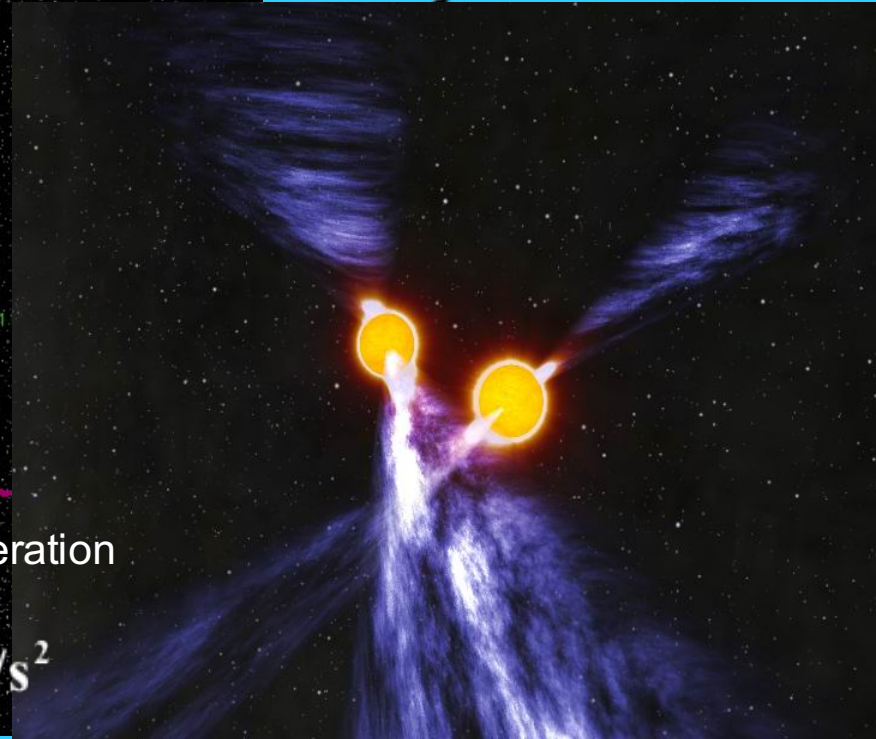
## Pioneer anomaly



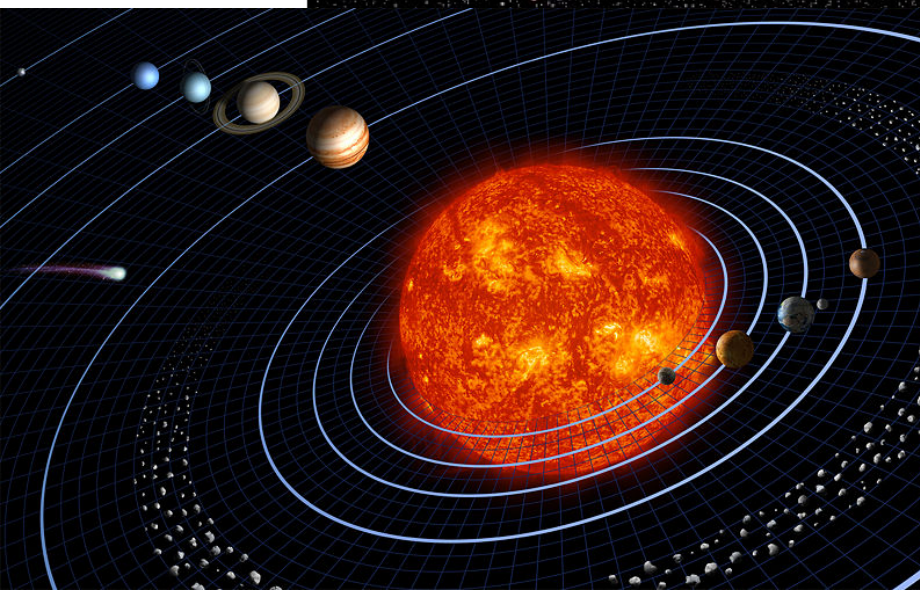
Pioneer 10	Blue
Pioneer 11	Green
Voyager 1	Purple
Voyager 2	Red

Additional Solar-/Earth- ward acceleration for both spacecrafts

$$\Delta a = (8.74 \pm 1.33) \times 10^{-10} \text{ m/s}^2$$

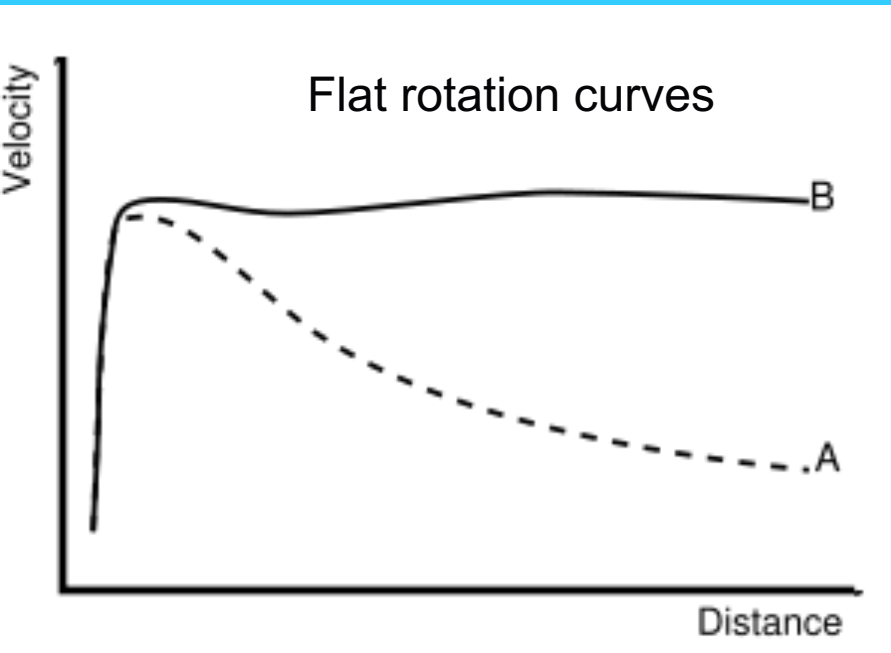


Extreme relativistic pulsar  
PSR B1913+16

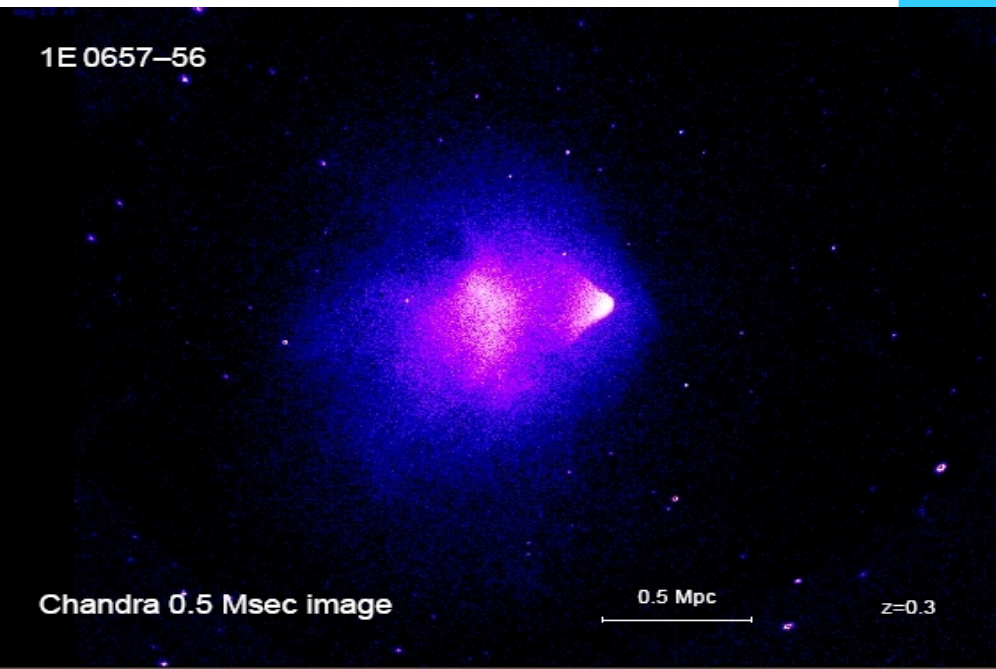


Kepler's Law  
of planetary  
motion

# Tests on the scale of Galaxies

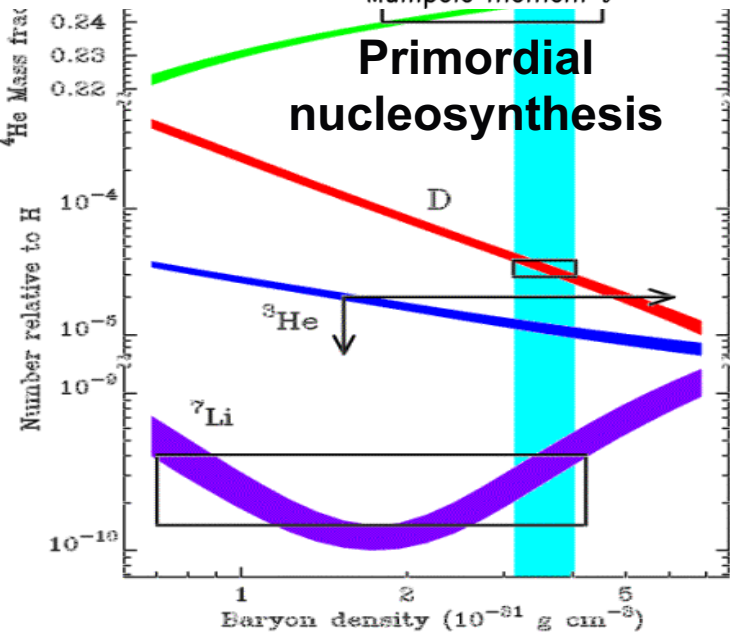
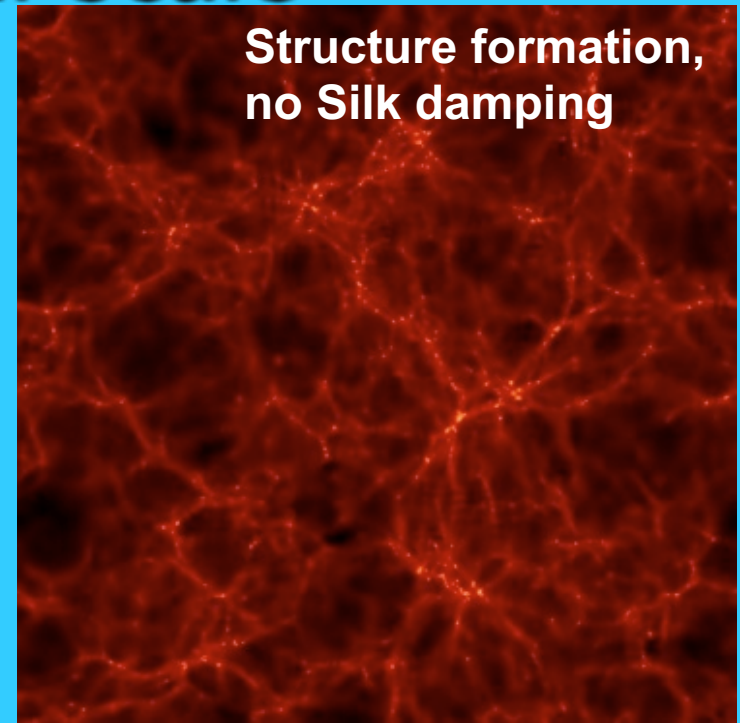
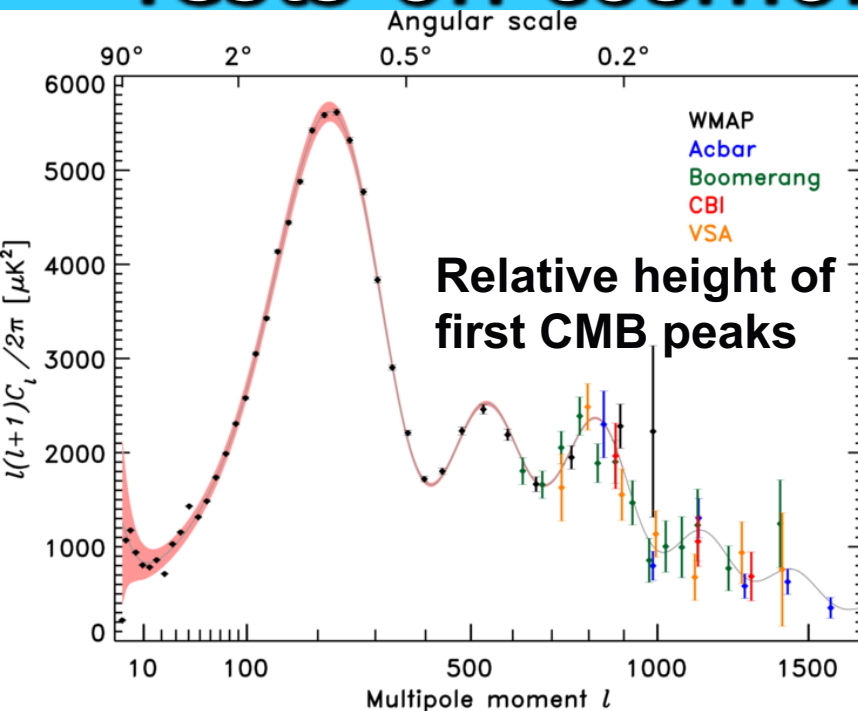


Rotation curves in dwarf Galaxies may require different fit parameters

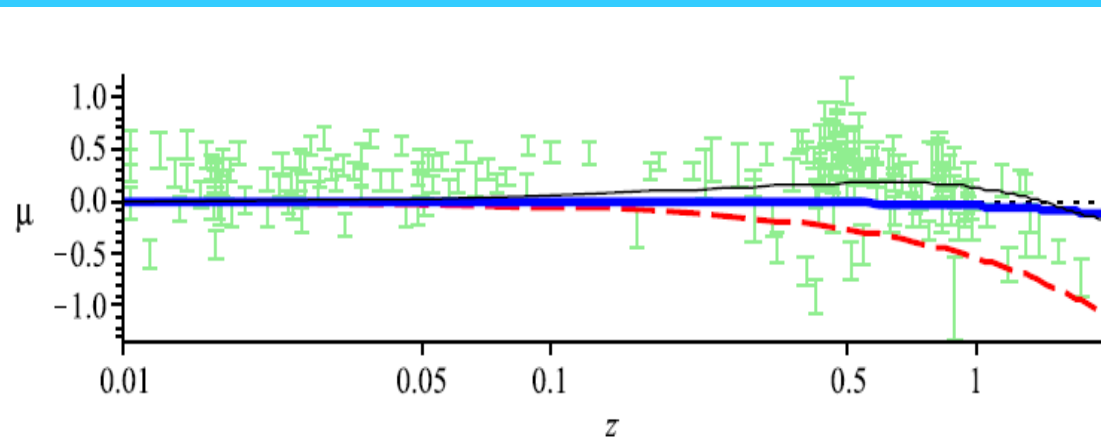


Unusual shape and high velocities in Bullet Cluster

# Tests on cosmological scale



Accelerating expansion of the Universe?



- More generally, searches for deviations in the PPN-like parameter, on cosmological scales.

- A real opportunity with future surveys: satellites (Euclid, JDEM), groundbased (SKA, LSST, ...).

# Conclusions:

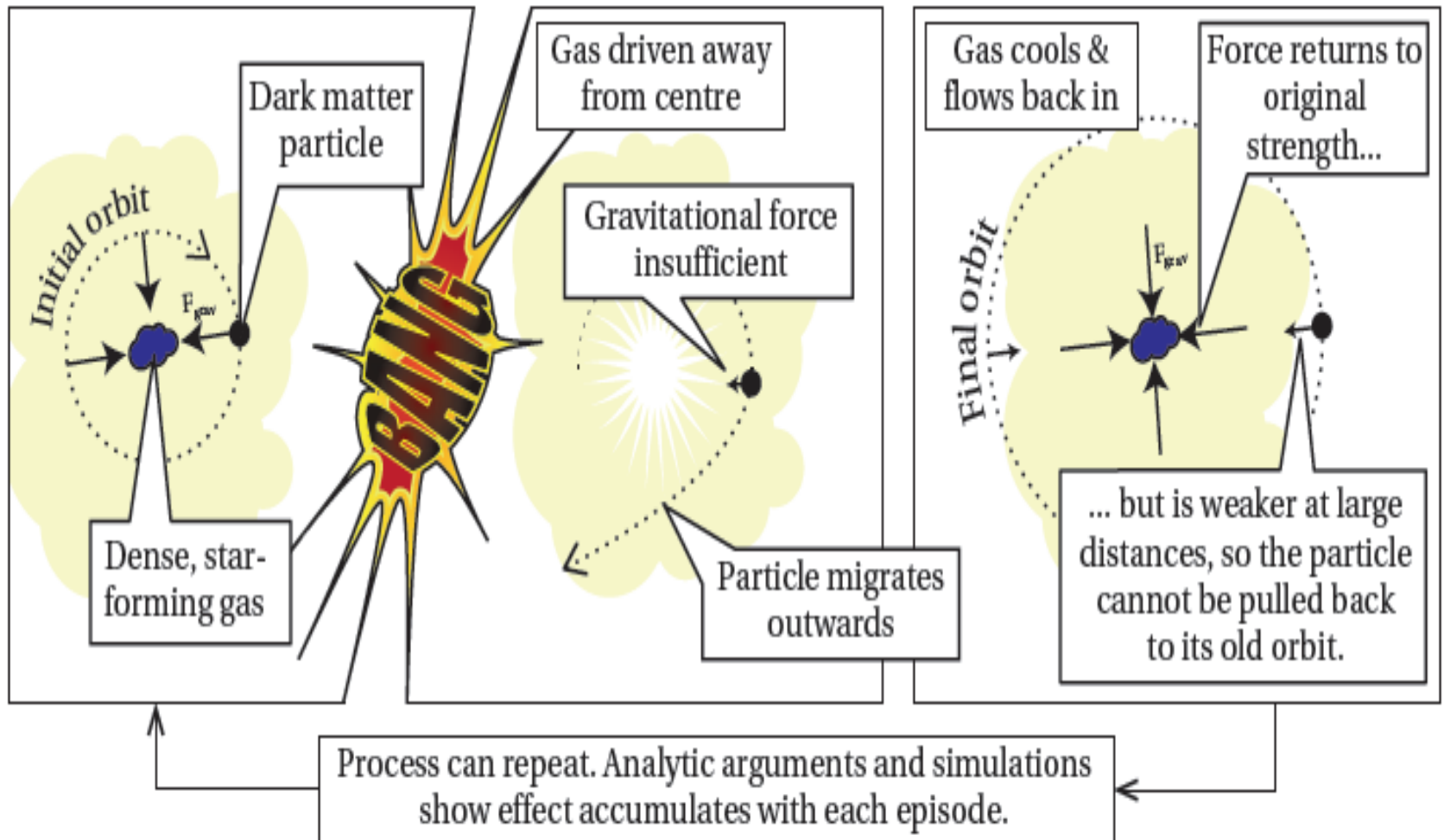
- Does Einstein/Newton gravity break down in regions of very weak field?
- Is there a consistent theory for this deviation from standard gravity?
- How can we test it, i.e. how can we distinguish it from dark matter models?

# Astrophysical solutions

# How baryons affect DM through gravity

· how gas affects dark matter through gravity

Supernovae Feedback



Navarro et al. 1996; Gelato & Sommer-Larsen 1999; Read & Gilmore 2005; Mashchenko+2006, 2008; Governato+2010, 2012; Pontzen & Governato 2011; Pontzen & Governato 2014

# SUPERNOVAE FEEDBACK

- **Simulations** (Navarro et al. 1996; Gelato & Sommer-Larsen 1999; Read & Gilmore 2005; Mashchenko+2006, 2008, Governato+2010, 2012; Teyssier+2012):
- Energetic feedback generates large underdense bubbles of expanding gas from centrally-concentrated bursts of star formation (3 Myr).
- The potential in the central kiloparsec changes on sub-dynamical timescales (25 Myr) over the redshift interval  $4 > z > 2$ .
- Gas outflows from supernovas remove the low angular momentum gas, stopping bulge formation and decreasing the central DM
- In the inner 1 kpc the density is less than  $\frac{1}{2}$  of that in absence of outflows
- **Result:** LSBs with DM core
- **Theoretical model** (Pontzen & Governato 2011): supply of gas+collapse & rapid expansion  $\longrightarrow$  fluctuations in the central potential  $\longrightarrow$  irreversible transfer energy into collisionless particles  $\longrightarrow$  dark matter core if central starbursts or AGN phases are sufficiently frequent and energetic.

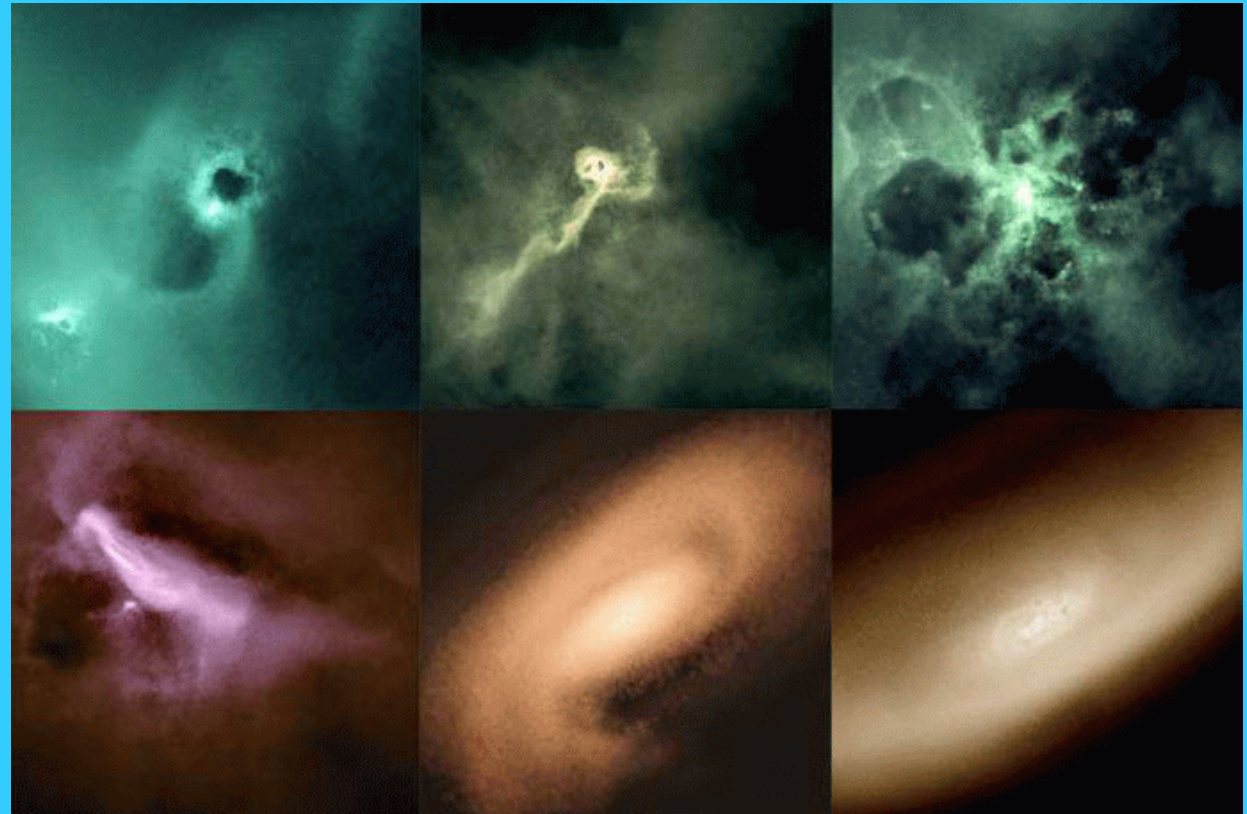
# High-res dwarf galaxy formation simulation

Governato, Brook, Mayer  
et al., *Nature*, Jan 14, 2010 (G10)

$V_{c,halo} \sim 50$  km/s  
 $N_{SPH} \sim 2 \times 10^6$  particles  
 $N_{dm} \sim 2 \times 10^6$  particles  
( $M_{sph} \sim 10^3$  Mo)  
spatial resolution  
(grav. softening) 75 pc

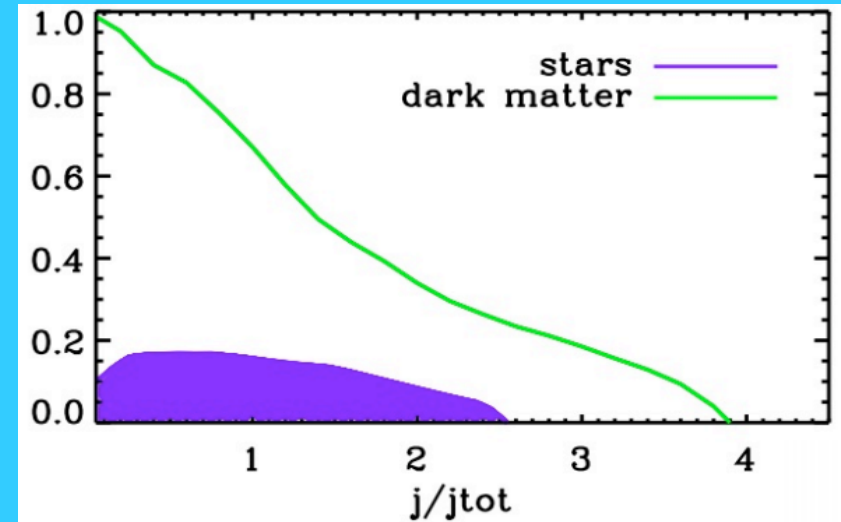
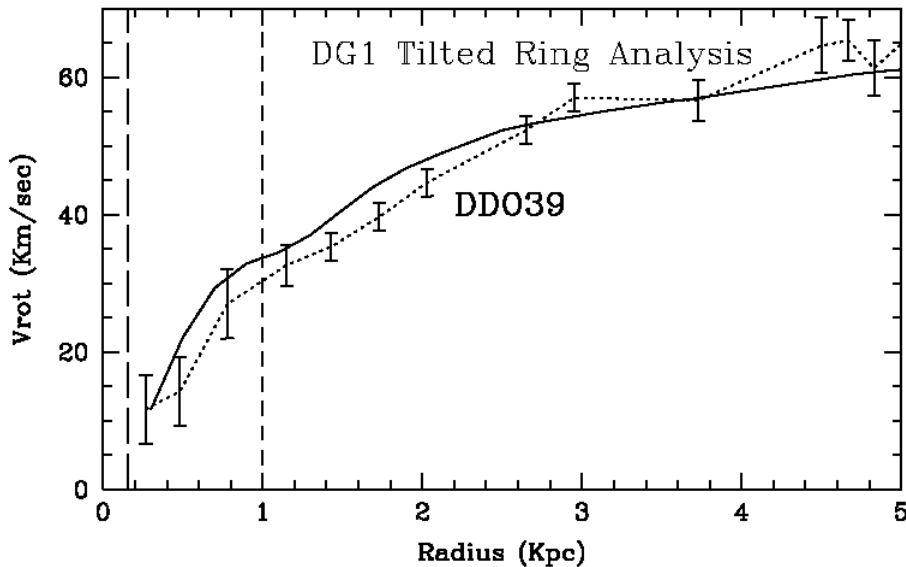
- High SF threshold  
100 atoms/cm<sup>3</sup>  
(highest physical density  
at G10 resolution)

- Supernovae blastwave  
feedback model with  
same parameters as in  
previous MW-sized  
galaxies simulations



The formation of a dwarf, bulgeless galaxy. Blue maps the gas density, while stars are shown in red/white/blue depending on their age (blue stars are younger and brighter) 1 second represents about 100 million years in real time.

-> and produce a slowly rising rotation curve!



How? Removal of baryons (**baryonic disk mass fraction  $\sim 0.03$  at  $z=0$ , so 5 times lower than cosmic  $f_b$** ) + flattening of dark matter profile

During strongest outflows (at  $z > 1$ ) inner dark matter mass expands as a result of impulsive removal of mass

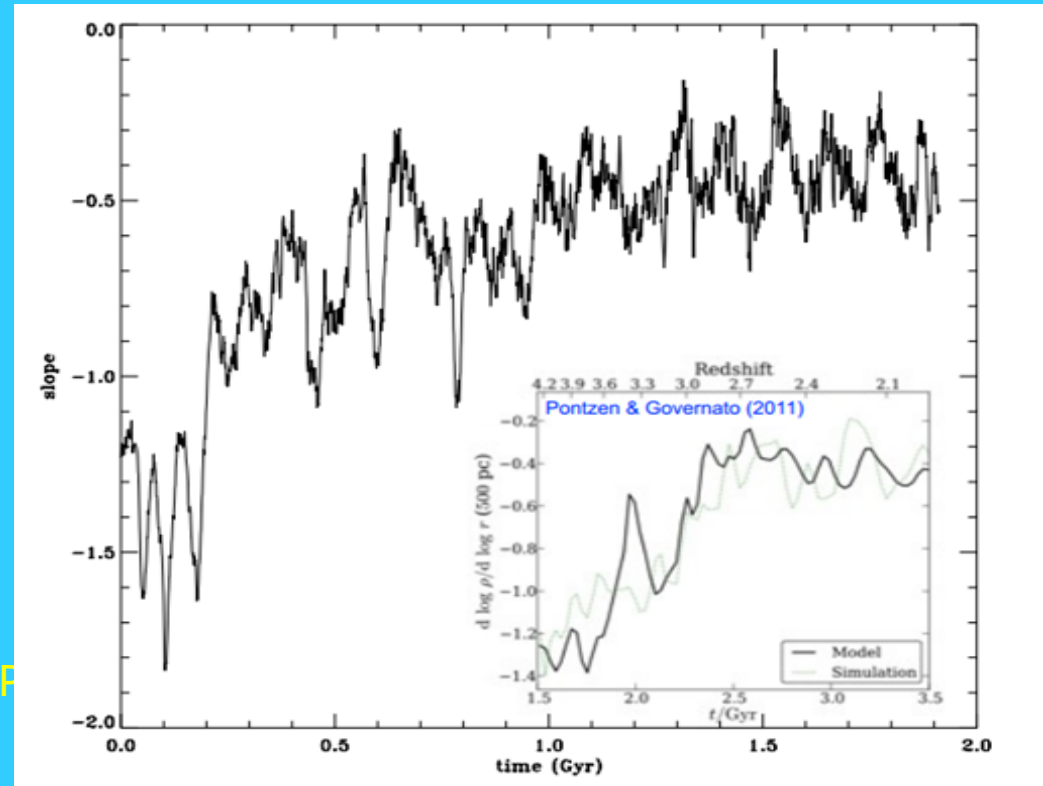
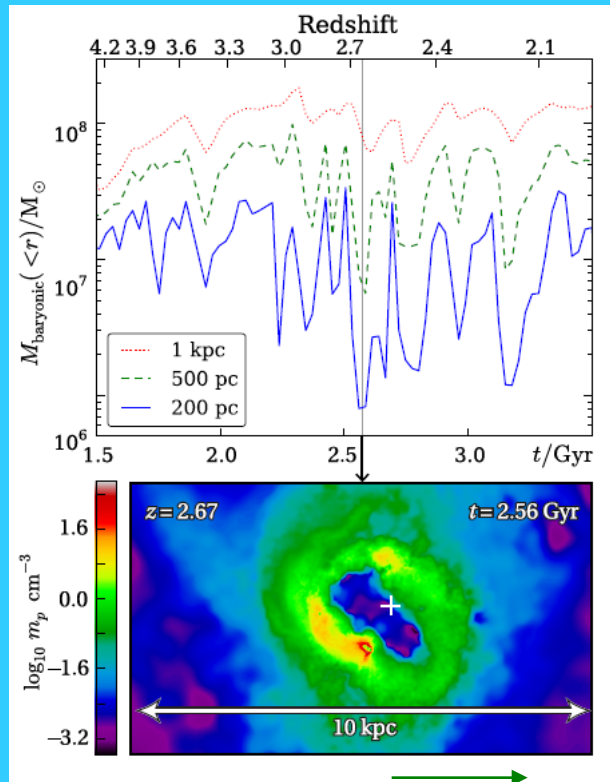
(confirms earlier models of e.g. Navarro et al. 1996; Read et al. 2003, etc)

Dark matter density decreases by a factor of  $\sim 2$  at  $r < 1$  kpc and density profile becomes shallower  $\sim r^{-0.6}$  rather than  $\sim r^{-1}$

# High density threshold SF in dwarfs

High resolution simulation with dense clumps and strong feedback result in very strong and very fast potential variations (Navarro et al. 1996; Gelato & Sommer-Larsen 1999; Read & Gilmore 2005; Mashchenko+2006, 2008, Governato+2010, 2012; Pontzen & Governato 2011; Teysnier+2012)

Fluctuations in the central potential -> Irreversible "heating" of DM cusp into core



Top panel: Baryonic mass in 1 kpc, 500 pc, 200 pc (from top to bottom). Bursty star formation+SF rapid, coherent oscillations in the potential  $t_{\text{orb,DM}}(1 \text{ kpc}) \sim 25 \text{ Myr}$ . Supernovae bubbles encompass the 1kpc in 3 Myr

Bottom Panel: disk plane density during the starburst event at 2.56 Gyr. An underdense bubble formed at disk center through the thermal expansion of the gas heated by SF explosion

# ALTERNATIVE APPROACH TO N-BODY SIMULATIONS

- Controversy regarding central slope and universality of the density profile has stimulated several analytical works : **Gunn & Gott's SIM** (Ryden & Gunn 1987; Avila-Reese 1998; DP2000; Lokas 2000; Nusser 2001; Hiotelis 2002; Le Delliou Henriksen 2003; Ascasibar et al. 2003; Williams et al. 2004; Del Popolo 2009).
- Del Popolo 2000, Lokas 2000 reproduced the NFW profile considering radial collapse. SIM is improved by calculating the initial overdensity from the perturbation spectrum and eliminating limits of previous SIM's works.
- Other authors studied the effect of angular momentum,  $L$ , and non-radial motions in SIM showing a flattening of the inner profile with increasing  $L$ .
- El-Zant et al. (2001) proposed a semianalytical model: dynamical friction dissipate orbital energy of gas distributed in clumps depositing it in dark matter with the result of erasing the cusp.

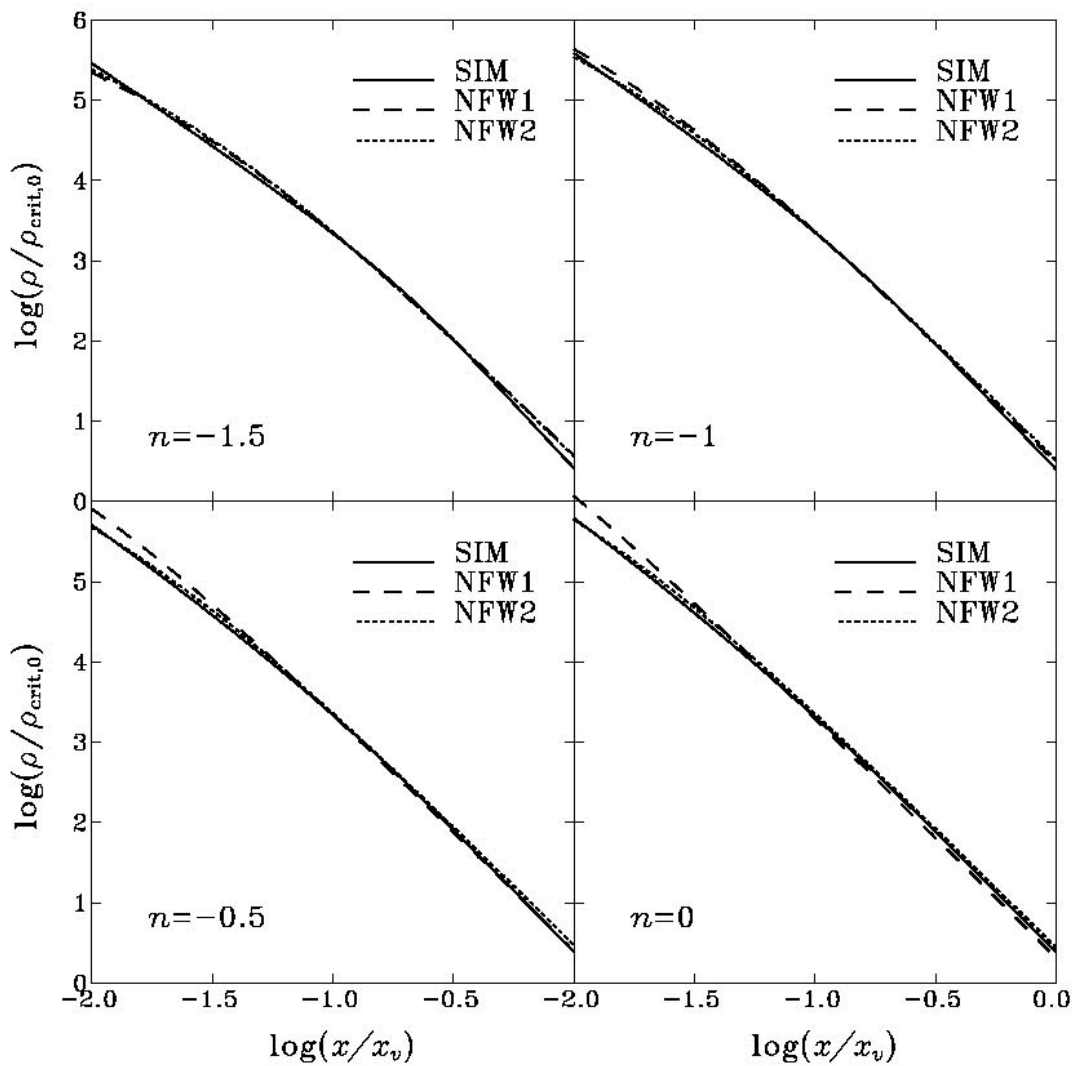


Figure 3. The density profiles of dark matter halos of mass of the order of  $0.02M_*$ , for different spectral indices  $n$  in the range  $0.01x_v < x < x_v$ . The solid lines show the predictions of SIM. The long-dashed ones give the NFW results with their fitted concentrations, while the short-dashed curves present the NFW formula (39) with concentrations fitted to SIM results.

\*

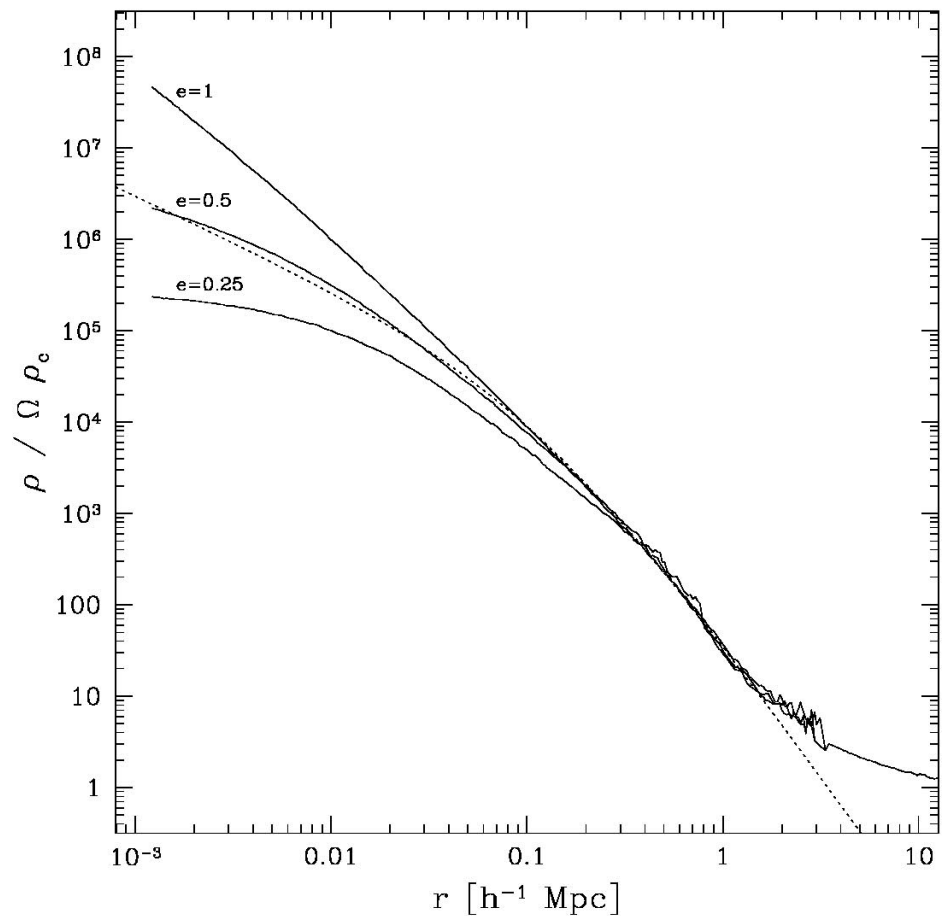
Lokas 2000;  
 scale free  
 spectrum  
 •Improvement  
 of Hoffman-Shaham  
 model.  
 •Radial collapse

NFW1: values of  $c_{vir}$  calculated  
 from a model based  
 on merging  
 formalism provided  
 by NFW that describes  
 better their N-body  
 Simulations.

NFW2:  $c$  is obtained  
 from NFW fitting  
 formula

\*

- Ascasibar et al. 2003 (radial density profile from a 3 sigma fluctuation on 1 h<sup>-1</sup> Mpc scale).
- Angular momentum introduced as the eccentricity parameter
- Changing the orbit eccentricity  $e$  (proportional to  $L$ ) produces a flattening of the inner profile. Radial orbits gives rise to a steep profile similar to that proposed by Moore et al. (1999)
- Numerical experiments, in the same paper shows that central slopes in relaxed haloes could be less steep than the NFW fit in agreement with analytical models based on the velocity dispersion profile (Taylor & Navarro 2003; Hoefl et al. 2003)



\* Williams et al. (2004)

• Follows Ryden & Gunn (1987): only random angular momentum is taken into account

• More massive galaxy halos tend to be more centrally concentrated, and have flatter rotation curves

• Specific angular momentum (only random L) in Williams haloes is less centrally concentrated and larger than in N-body simulations (e.g. van den Bosch et al. 2002).

• In order to reproduce a NFW profile one has to reduce random velocities by a factor of two. As suggested by Williams haloes in N-body simulations lose angular momentum between 0.1 and 1  $R_{\text{vir}}$ . It is well known that numerical haloes have too little angular momentum vs. real disk galaxies (L catastrophe)

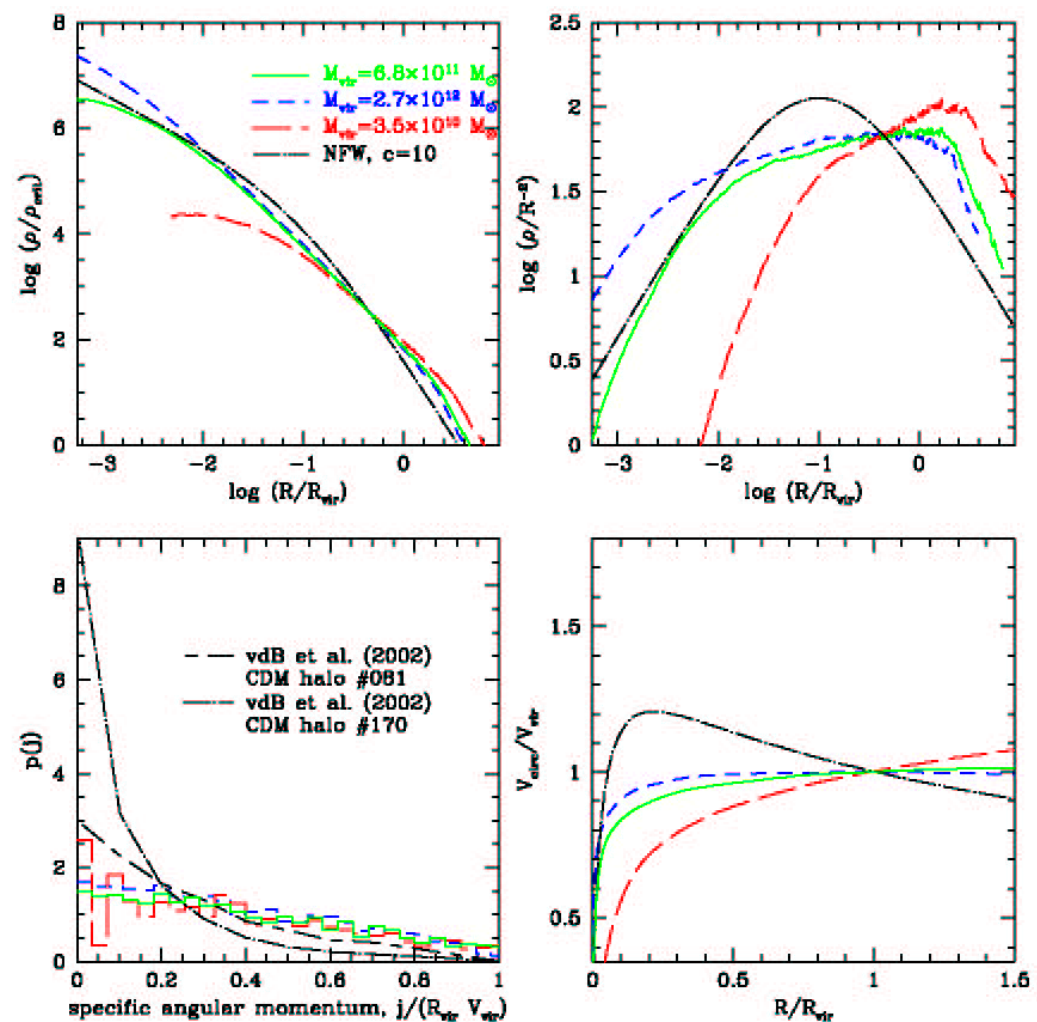


Fig. 1.— Dark matter halos generated using “standard” initial conditions, as described in Section 4.3. Halos of three different galactic-type masses are shown; the intermediate mass halo (solid line) is the ‘reference’ halo. *Upper left*: log-log density profiles. The lowest mass halo is not resolved at  $\lesssim 1\%$  of  $R_{\text{vir}}$ . NFW  $c = 10$  halo is shown for comparison (dot-dash line). *Upper right*: density profiles with the slope of  $\alpha = 2$  divided out, so  $\alpha = 2$  slopes are flat in this plot. *Lower right*: circular rotation curves. *Lower left*: the distribution of specific angular momenta (SAM) in our halos, as histograms. For comparison, we include two extreme SAM distributions taken from N-body simulations of van den Bosch *et al.* (2002).

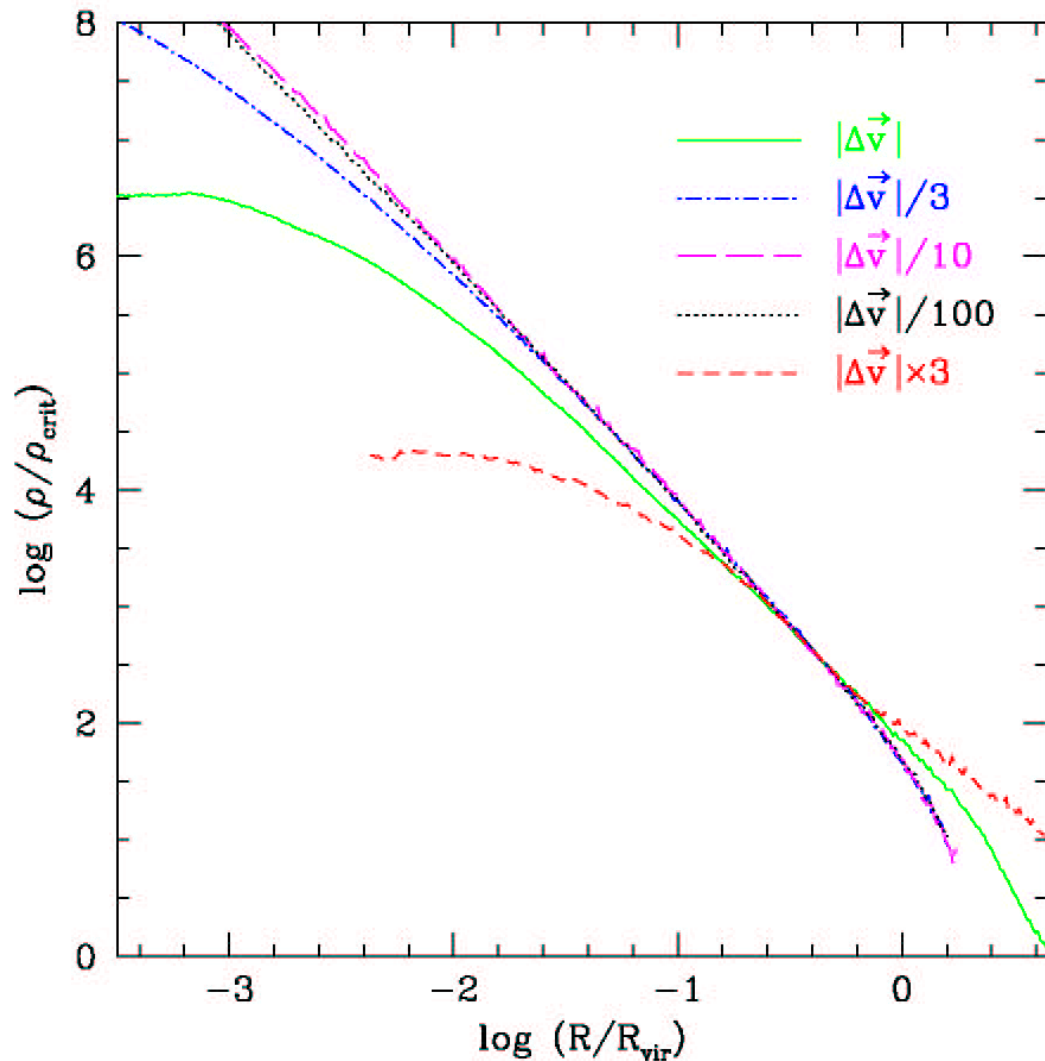


Fig. 6.— Density profiles of halos whose random particle velocities have been reduced by factors of 3 (dot-dash), 10 (long dash) and 100 (dotted), and increased by a factor of 3 (short dash), compared to the reference halo (solid line). Reducing random velocities means that the angular momentum of dark matter particles is reduced, which results in steeper central density slopes. The limiting slope,  $\alpha = 2$  is discussed in Section 5.1, and the progressive shallowing of the slopes in Section 5.3.

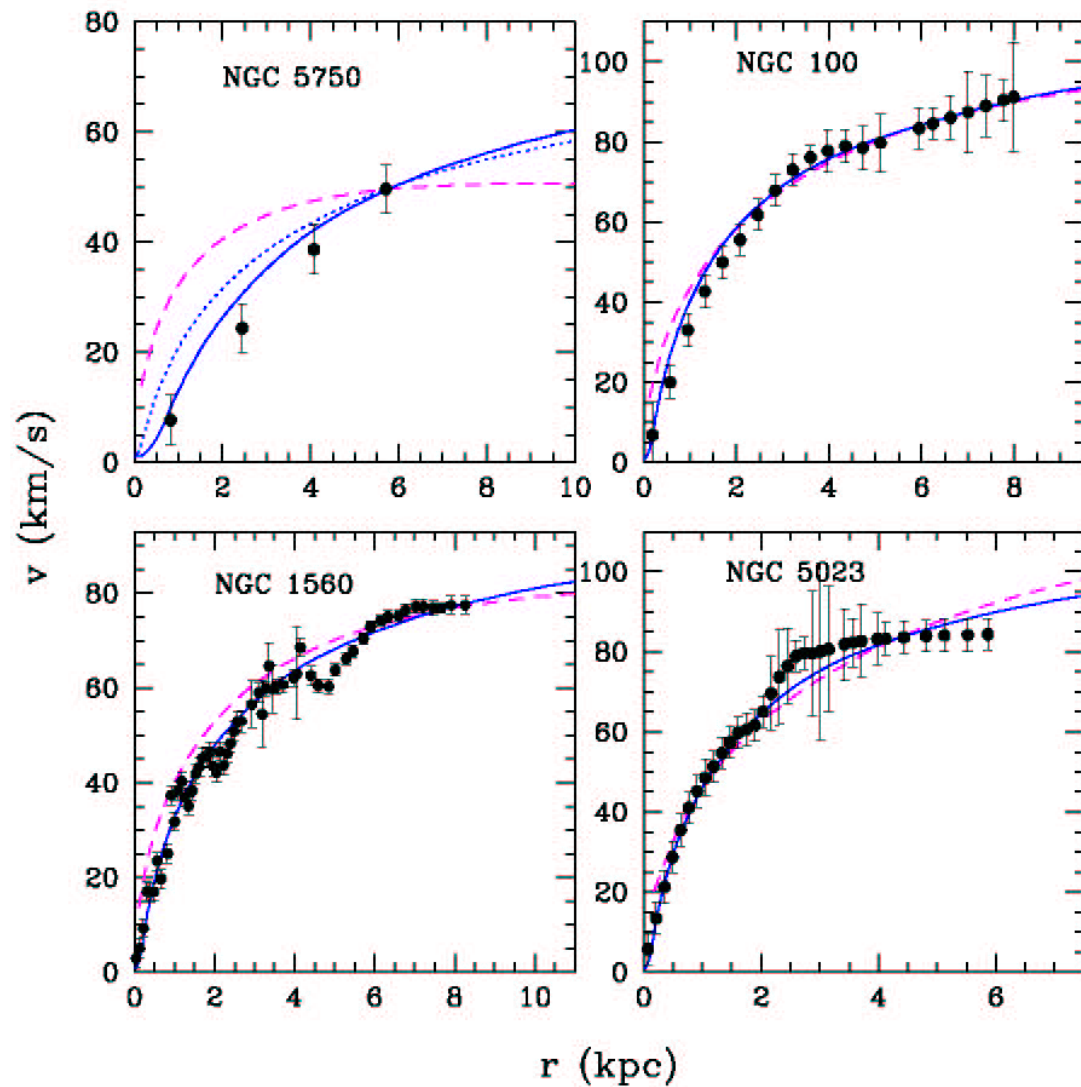


Fig. 5.— The points with error-bars are the high-resolution rotation curves of LSB galaxies taken from de Blok & Bosma (2002). The dashed lines are NFW fits obtained by adjusting 1 parameter:  $c$  varies between 13.5 and 17 for these galaxies. The solid lines are our halos with tangentially oriented velocity ellipsoids:  $\zeta_0 = 20^\circ$  for NGC 5750 and NGC 100, and  $\zeta_0 = 50^\circ$  for NGC 1560 and NGC 5023. The dotted curve in the upper left represents our halo with a spherical velocity ellipsoid, i.e.  $\zeta_0 = 90^\circ$ . See Section 4.7 for details.

# Baryonic clumps+DF (El-Zant+ 2001, 2004, Cole+ 2011...)

- Spherical Halo containing  $N_{\text{DM}}$  particles of DM of mass  $M_{\text{DM}} + N_{\text{g}}$  particles (baryonic clumps) of mass  $M$  (baryonic fraction 10% of total mass of the system; mass of clumps  $\Rightarrow > 0.1\% M_{\text{total}}$ ). A system of  $10^5$  particles is divided into a  $10^3$  equal number bins
- Baryonic clumps suffer dynamical friction, described by the Chandrasekhar formula, and the energy lost is redistributed among the dark matter particles using a Monte Carlo technique

$$\left(\frac{d\mathbf{V}_M}{dt}\right)_{\text{DF}} = -\frac{4\pi G^2 \ln \Lambda \rho M}{V_M^3} \left(\text{erf}(X) - \frac{2X}{\sqrt{\pi}} \exp[-X^2]\right) \mathbf{V}_M$$

$$\Lambda = bV_M^2 / G(M + m)$$

- $X = V_M / 2^{0.5}$  ,  $M = M_{\text{DM}} \ll M$

- The energy lost by the gas particles of mass  $M$  and velocity  $V_M$  in a timestep  $\Delta t$  in a given bin

$$E_{lostbin} = \Sigma_{bin} M \left( \frac{d\mathbf{V}_M}{dt} \cdot \mathbf{V}_M \right) \Delta t$$

- is gained as random kinetic energy by the halo particles in the same bin

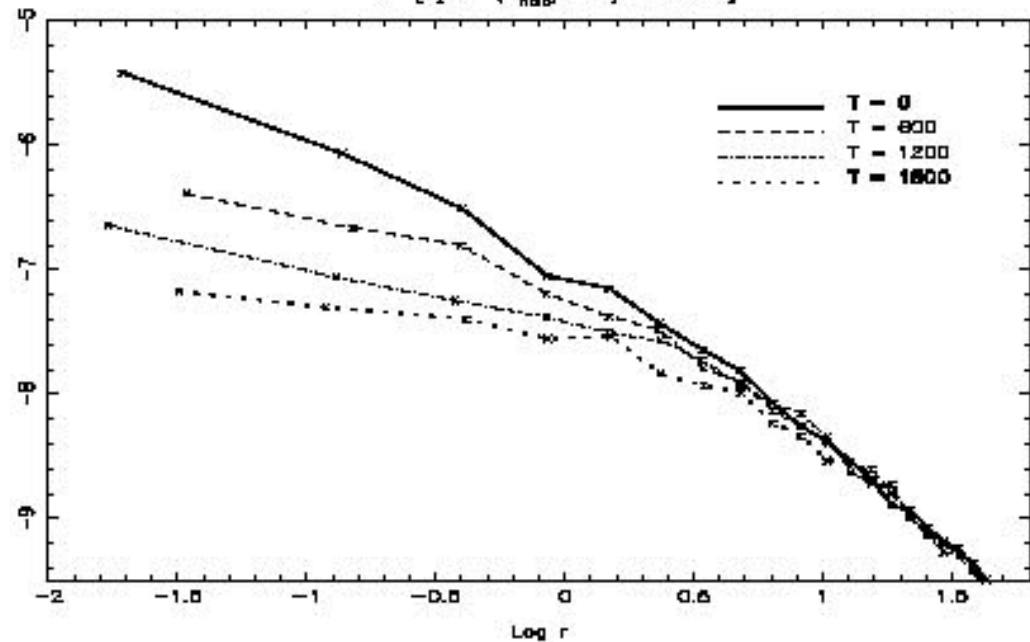
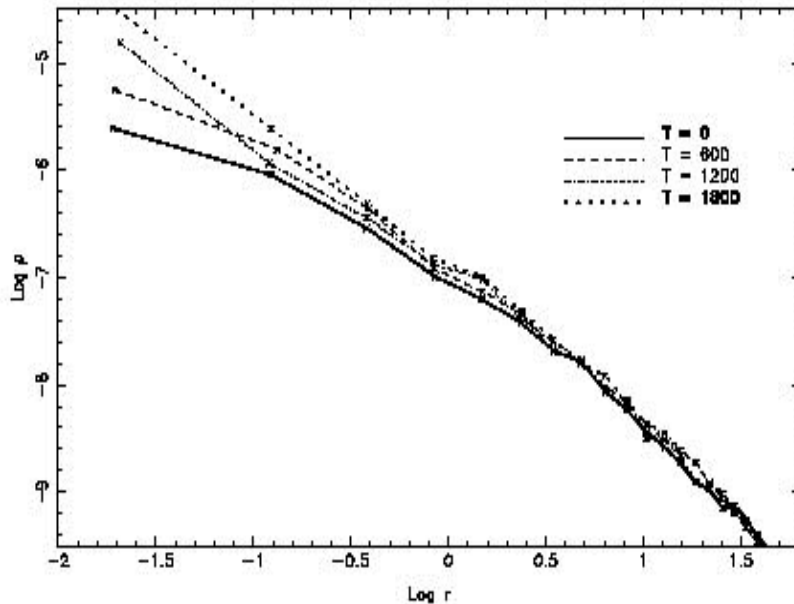
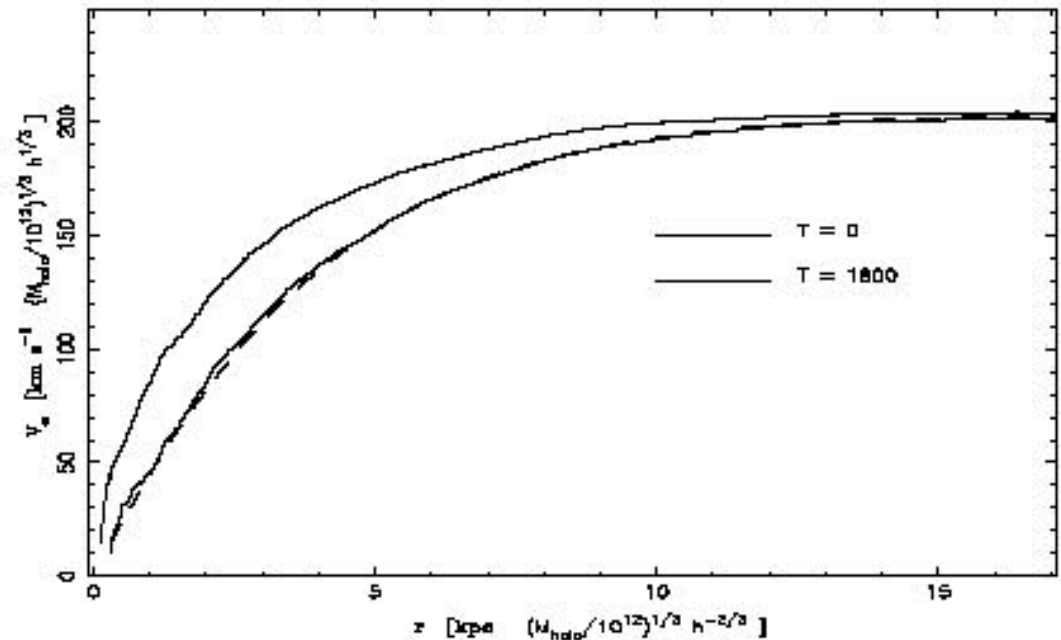
$$V_i \rightarrow V_i + F(y)$$

$$y = \sqrt{(2/3)E_{lostbin}/m_{bin}},$$

where  $F$  is a normal distribution of zero mean and variance and  $m_{bin}$  represents the CDM mass in a given bin

- Initially DM and baryons have a NFW distribution.
- The velocities are determined by solving the Jeans equation and are sampled from a Maxwellian distribution

- El-Zant et al. 2003.
- Transfer of energy from baryons to DM by DF.
- Initial and final DM rotation curve and profile. Dashed line is a fit using Burkert profile.
- Bottom left: DM profile in absence of energy feedback.



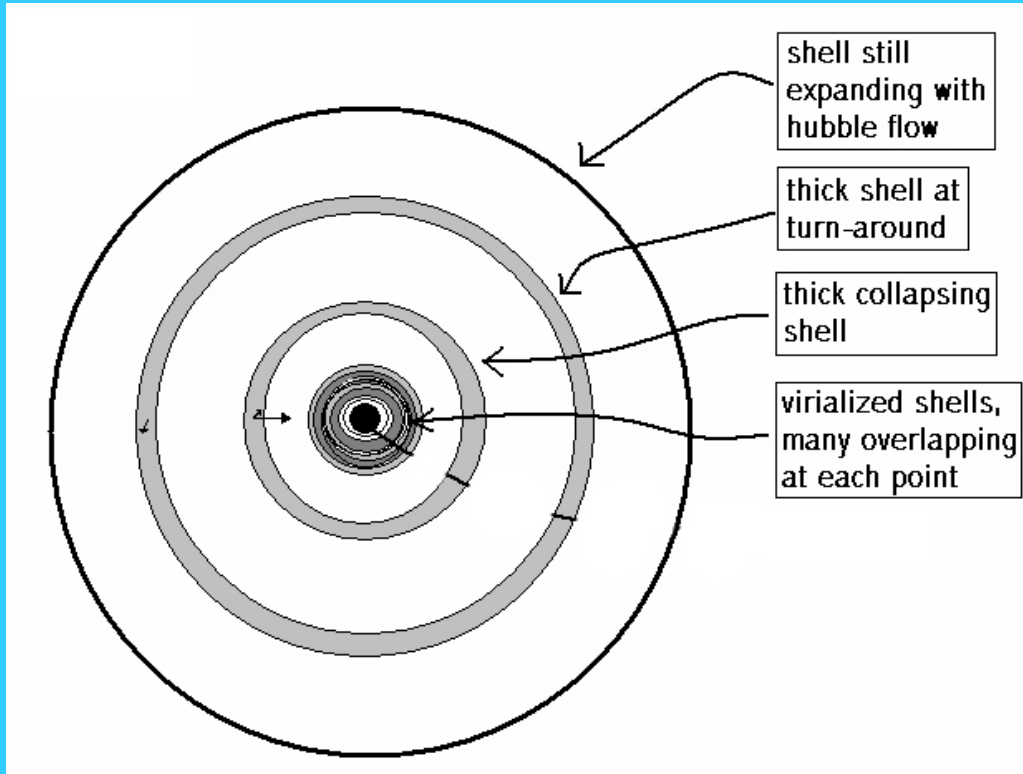
# Baryonic clumps+DM+DF+L

- As already described: exchange of angular momentum among baryonic clumps and DM

Simulations study only the Cusp/Core problem (El-Zant et al. 2001, 2004; Ma & Boylan-Kolchin 2004; Nipoti et al. 2004; Romano-Diaz et al. 2008, 2009; Cole et al. 2011; Inoue & Saitoh 2011).

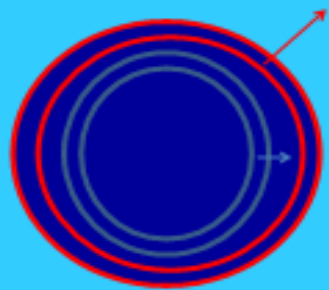
- Semi-analytical model (e.g., SIM) (DP09, 10; 11, 12, +14)

# How does SCM-SIM work?

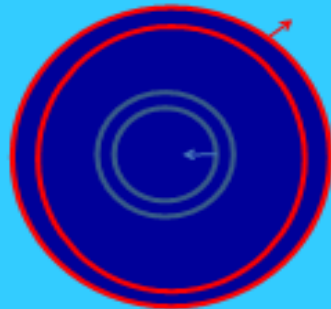


In the evolution of a density perturbation in the NL phase one may use semianalytical models (spherical or ellipsoidal collapse) (Gunn & Gott 1972; Gunn 1977; Bertschinger 1985; Hoffman & Shaham 1985; Ryden & Gunn 1987; Ascasibar, Yepes & Göttember 2004; Williams, Babul & Dalcanton 2004; DP09,10; Zukin & Bertschinger 2010)

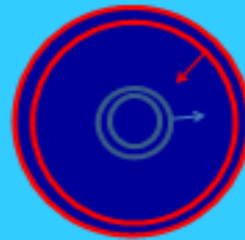
# How does SCM-SIM work?



Initial Hubble flow



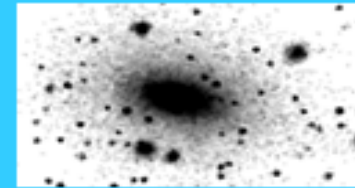
Collapsing,  
Inner shells reach  
The center earlier



Inner shells  
cross the center  
and move outward



Shell crossing,  
relaxation



Virialization,  
DM halo

$$\delta_1 = \rho(t_1)/\rho_b(t_1) - 1$$

$$M = \rho_b(4\pi r_1^3/3)(1 + \delta_1)$$

- A slightly overdense sphere, embedded in the Universe, is a useful non-linear model, as it behaves exactly as a closed sub-universe (if density is > critical density)
- The overdensity expands with Hubble flow till a maximum radius (**turn-around**). ( $r=r_{\max}$ ,  $dr/dt=0$ ) occurs at  $\delta_{lin} \sim 1.06$
- Then it **collapses** to a singularity. ( $r=0$ ):  $\delta_{lin} \sim 1.69$
- Collapse to a point will never occur in practice; dissipative physics and the process of **violent relaxation** will eventually intervene and convert the kinetic energy of collapse into random motions. This is named: **virialization** (occurs at  $2t_{\max}$ , and  $r_{vir} = r_{\max}/2$ )
- Once a non-linear object has formed, it will continue to attract matter in its neighbourhood and its mass will grow by accretion of new material (**secondary infall**).
- Through dissipative processes, baryons lose energy and fall deeper in the potential well of DM.
- If the cooling time of the baryon gas is smaller than the collapse time, fragmentation will take place and smaller units can collapse

# The Model: SIM + L+DF+DC (Del Popolo 2009, 2011, 2012)

- A bound mass shell having initial comoving radius  $r_i$  will expand to a maximum radius  $r_m$  (apapsis) of a shell:

$$r_m = g(r_i) = r_i \frac{1 + \bar{\delta}_i}{\bar{\delta}_i - (\Omega_i^{-1} - 1)} \quad \text{Eq. 1}$$

where

$$\bar{\delta}_i = \frac{3}{r_i^3} \int_0^{r_i} \delta(y) y^2 dy \quad \text{Eq. 2}$$

If mass is conserved and each shell is kept at its turn-around radius, then the shape of the density profile is given by (Peebles 1980; HS; White & Zaritsky 1992):

$$\rho_{ta}(r_m) = \rho(r_i) \left( \frac{r_i}{r_m} \right)^2 \frac{dr_i}{dr_m} \quad \text{Eq. 3}$$

After turn-around, a shell collapse, reexpands, recollapse (oscillation). This shell will cross other shells collapsing and oscillating like itself.

- ➔ Energy is not conserved and it is not an integral of motion anymore
- ➔ dynamics studied assuming that the potential near the center varies adiabatically (Gunn 1977; Filmore & Goldreich 1984; Zaritski & Hoffman 1993)

**Total mass in r is**

$$m_T(r) = m_P(r) + m_M(r)$$

Eq. 4

$$m_M(r) = \int_r^{R_0} P(r, \xi) \frac{dm_P}{d\xi} d\xi$$

Eq. 5

and

$$P(r, \xi) = \int_0^r \frac{d\eta}{v(\eta, \xi)} / \int_0^\xi \frac{d\eta}{v(\eta, \xi)}$$

Eq. 6

The radial velocity is obtained by integrating the equation of motion of the shell:

$$\frac{dv_r}{dt} = \frac{h(r, v)^2}{r^3} - G(r) - \mu_* \frac{dr}{dt} + \frac{\Lambda}{3} r$$

Eq. 7

**Kandrup 1980**

**h (specific angular momentum)**

**$\mu_*$**  (specific coefficient of dynamical friction)

$$F = -\mu v = -\frac{4.44 G^2 m_a^2 n_a}{\langle v^2 \rangle^{3/2}} \log \left\{ 1.12 \frac{\langle v^2 \rangle}{G m_a n_a^{1/3}} \right\}$$

**L from  
TTT**

$$\tau(\mathbf{x}) = -\frac{GM_{sh}}{4\pi} \int \varepsilon(\mathbf{x}) \mathbf{x} \times \nabla \Phi(\mathbf{x}) d\Omega$$

$$L = \int \tau(\theta) \frac{dt}{d\theta} d\theta$$

DF

**Random angular momentum**

$$j \propto \sqrt{GM r_m}$$

or  $j\alpha$

$$e_0 = \left( \frac{r_{min}}{r_{max}} \right)_0$$

Avila-Resse et al (1998)

Adiabatic contraction of DM: Gnedin et al. 2004; Del Popolo 2009

Baryons cool and fall into their final mass distribution  $M_b(r)$ , initial distribution of L. DM particle at  $r_i$  moves to  $r < r_i$ . Adiabatic invariant->

$$r [M_b(r) + M_{dm}(r)] = r_i M_i(r_i)$$

\* **M<sub>i</sub>(r<sub>i</sub>) = initial mass distribution; M<sub>dm</sub>= final distribution of dissipationless halo particles**

**If there is no crossing ->**

$$M_{dm}(r) = (1 - F)M_i(r_i) \quad \text{Eq. 9}$$

**Eqs 8 and 9 can be solved to calculate the final radial distribution of halo particles:**

$$\rho(x) = \frac{\rho_{ta}(x_m)}{f(x_i)^3} \left[ 1 + \frac{d \ln f(x_i)}{d \ln g(x_i)} \right]^{-1} \quad \text{Eq. 10}$$

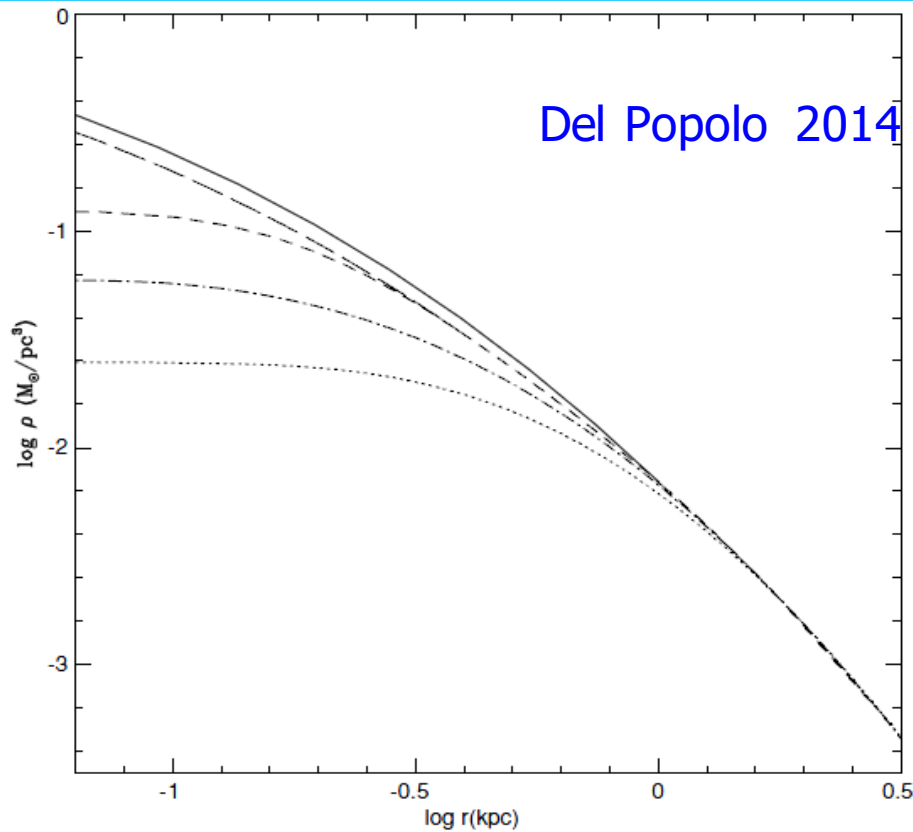
- **The collapse factor, f, of a shell with initial radius r<sub>i</sub> and apapsis r<sub>m</sub> is given by (Gunn 1977; FG84; ZH93):**

$$r = f(r_i)r_m = \frac{m_p(r_m)}{m_P(r_m) + m_M(r_m)}$$

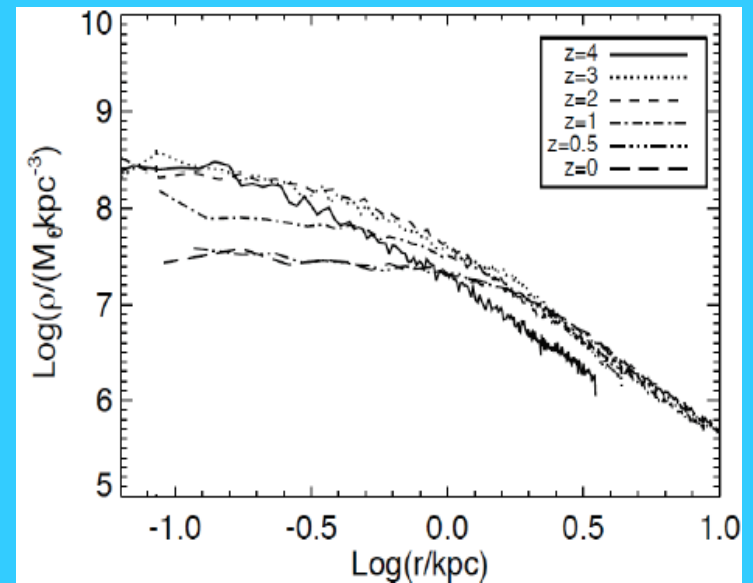
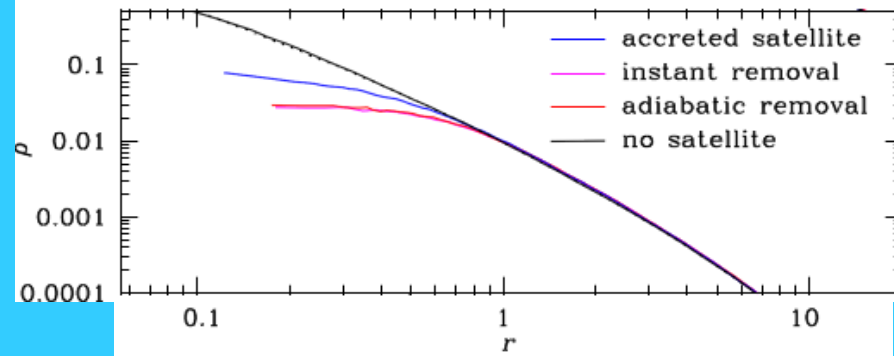
**The problem of determining the density profile is then solved fixing the initial conditions ( $\bar{\delta}_i$ ), the angular momentum h(r), and the coefficient of dynamical friction.**

# CUSP/CORE GALAXY DENSITY PROFILES

Del Popolo 2009  
 $z=10, 3, 2, 1, 0$

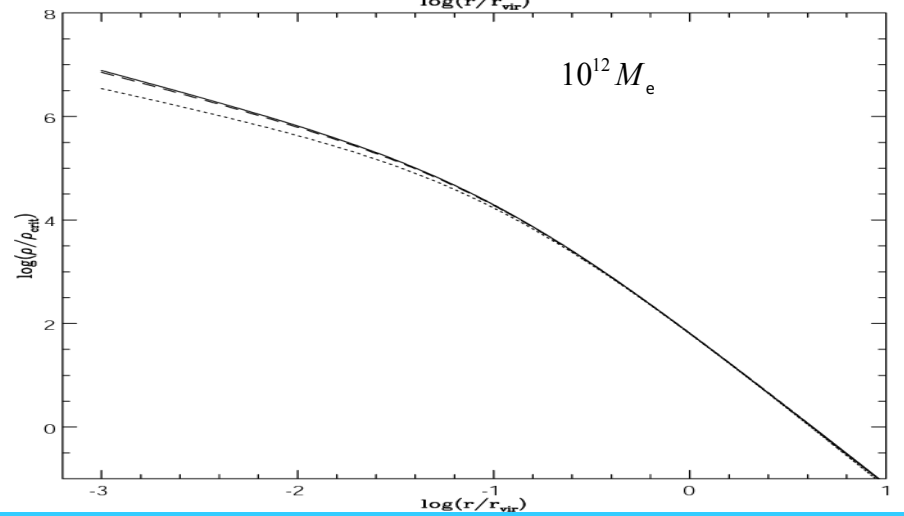
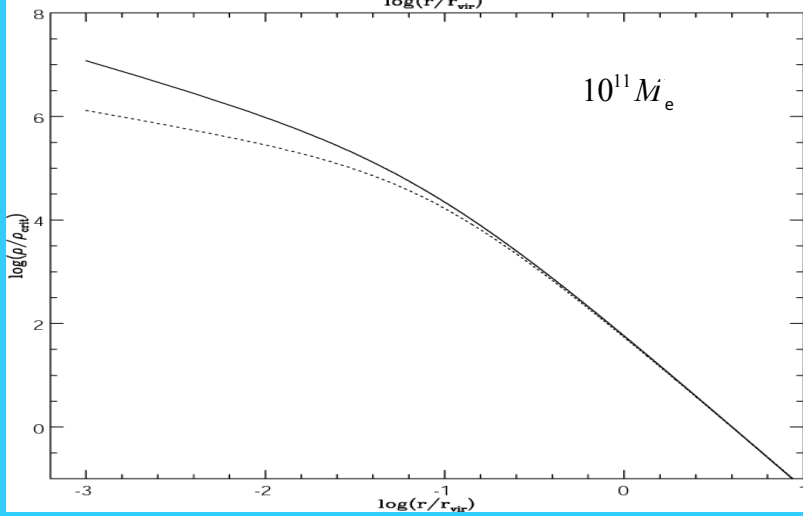
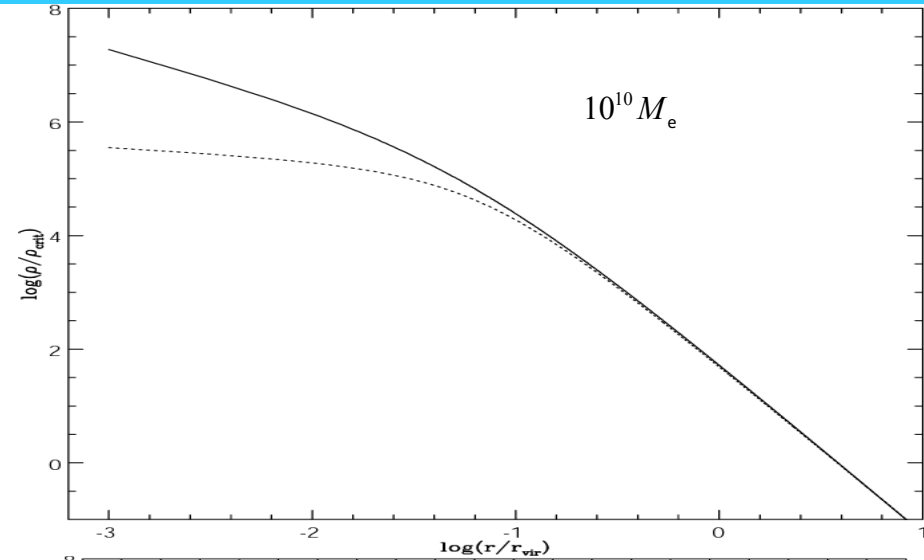
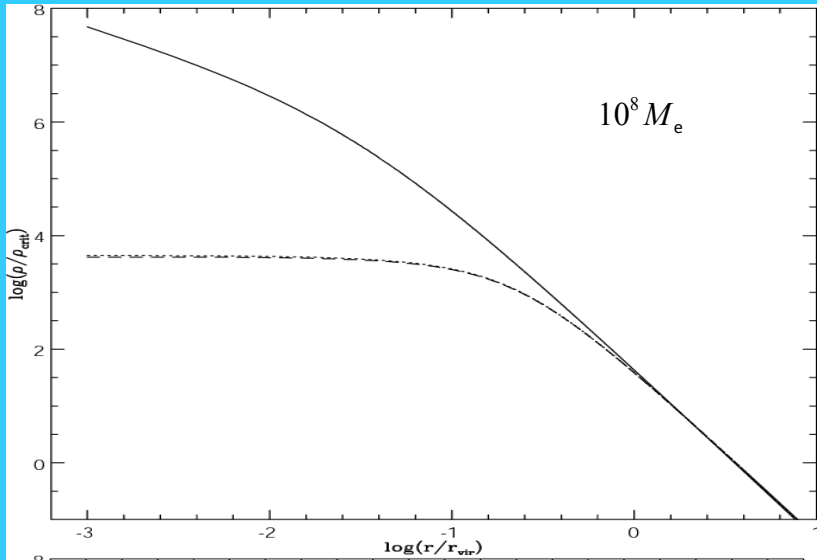


Cole+11

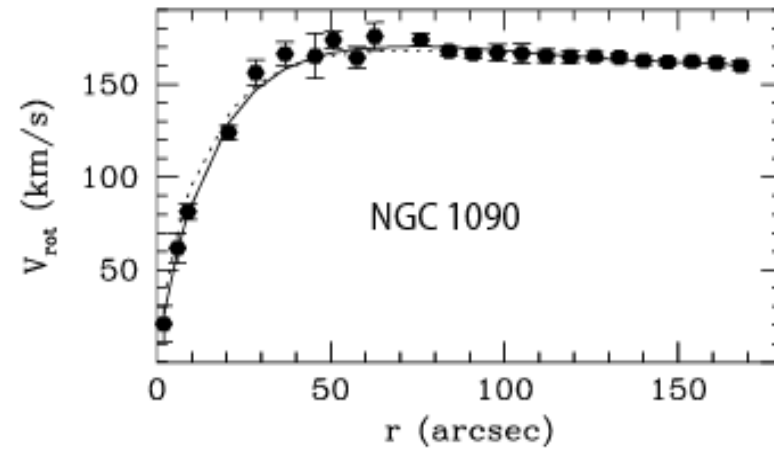
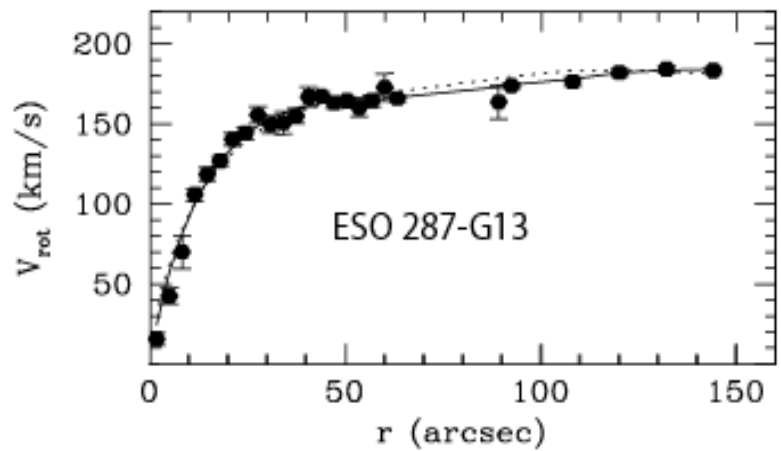
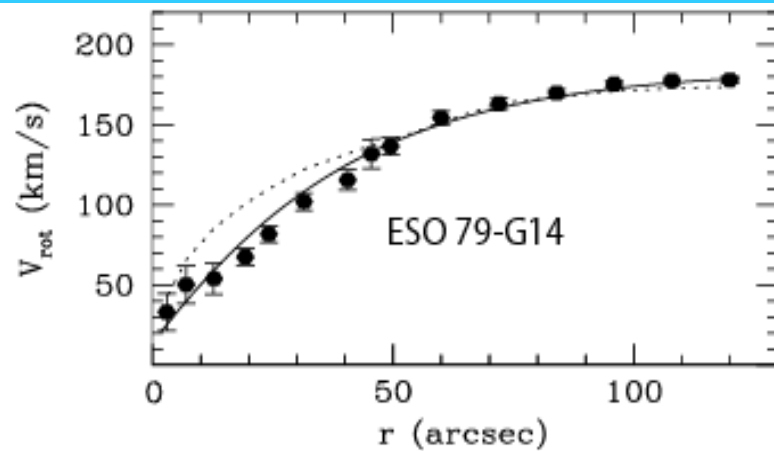
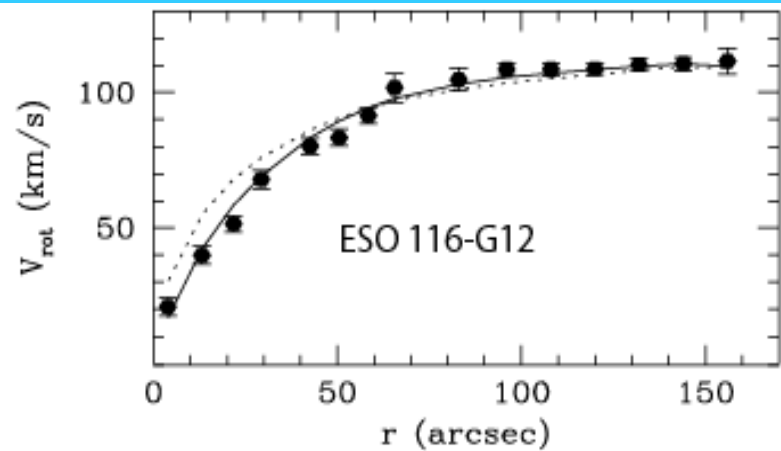


Governato+10

# CUSP/CORE GALAXY DENSITY PROFILES



\*



Rotation curves obtained with SIM (solid lines) and rotation curves of 4 LSBs Gentile et al. (2004). The dotted lines represent the fit with the NFW model

# Effect of Environment

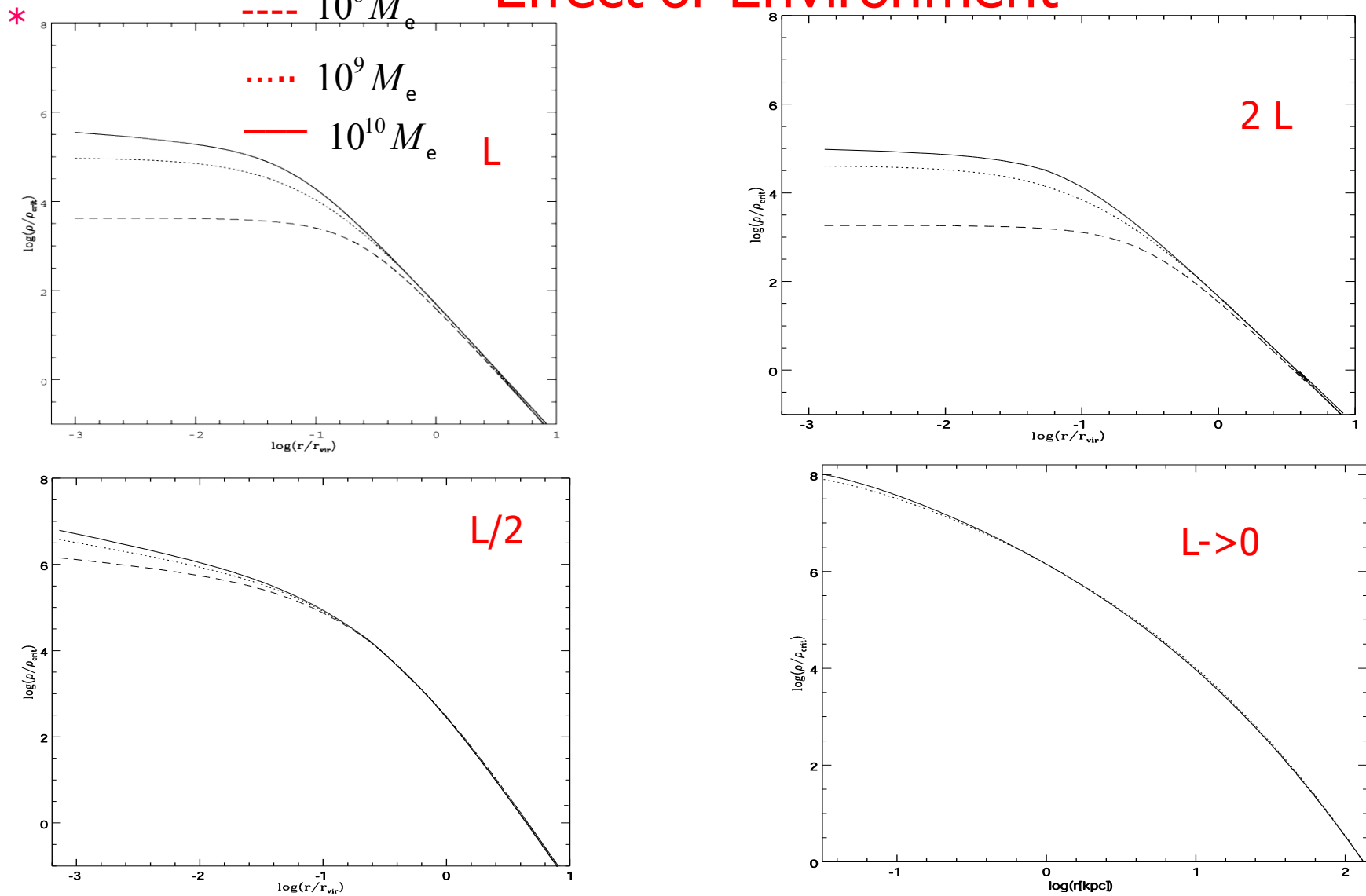


Figure 1. DM halos shape changes with angular momentum. DM haloes generated with the model of Section 2. In panels (a)(c), the dashed line, the dotted line and the solid line represent the density profile for a halo of  $10^8 M_{\text{sun}}$ ,  $10^9 M_{\text{sun}}$ , and  $10^{10} M_{\text{sun}}$ , respectively. In case (a), that is our reference case, the specific angular momentum was obtained using the tidal torque theory as described in Del Popolo (2009). The specific angular momentum,  $h$ , for the halo of mass  $10^9 M_{\text{sun}}$  is  $400 \text{ kpc km/s}$  ( $\text{spin} = 0.04$ ) and the baryon fraction  $f_d = 0.04$ . In panel (b) we increased the value of specific ordered angular momentum,  $h$ , to  $2h$  leaving unmodified the baryonic fraction to  $f_d$  and in panel (c) the specific ordered angular momentum is  $h/2$  and the baryonic fraction equal to the previous cases, namely  $f_d$ . Panel (d) shows the density profile of a halo of  $10^{10} M_{\text{sun}}$  with zero ordered angular momentum and no baryons (solid line), while the dashed line is the Einasto profile.

# Effect of Environment

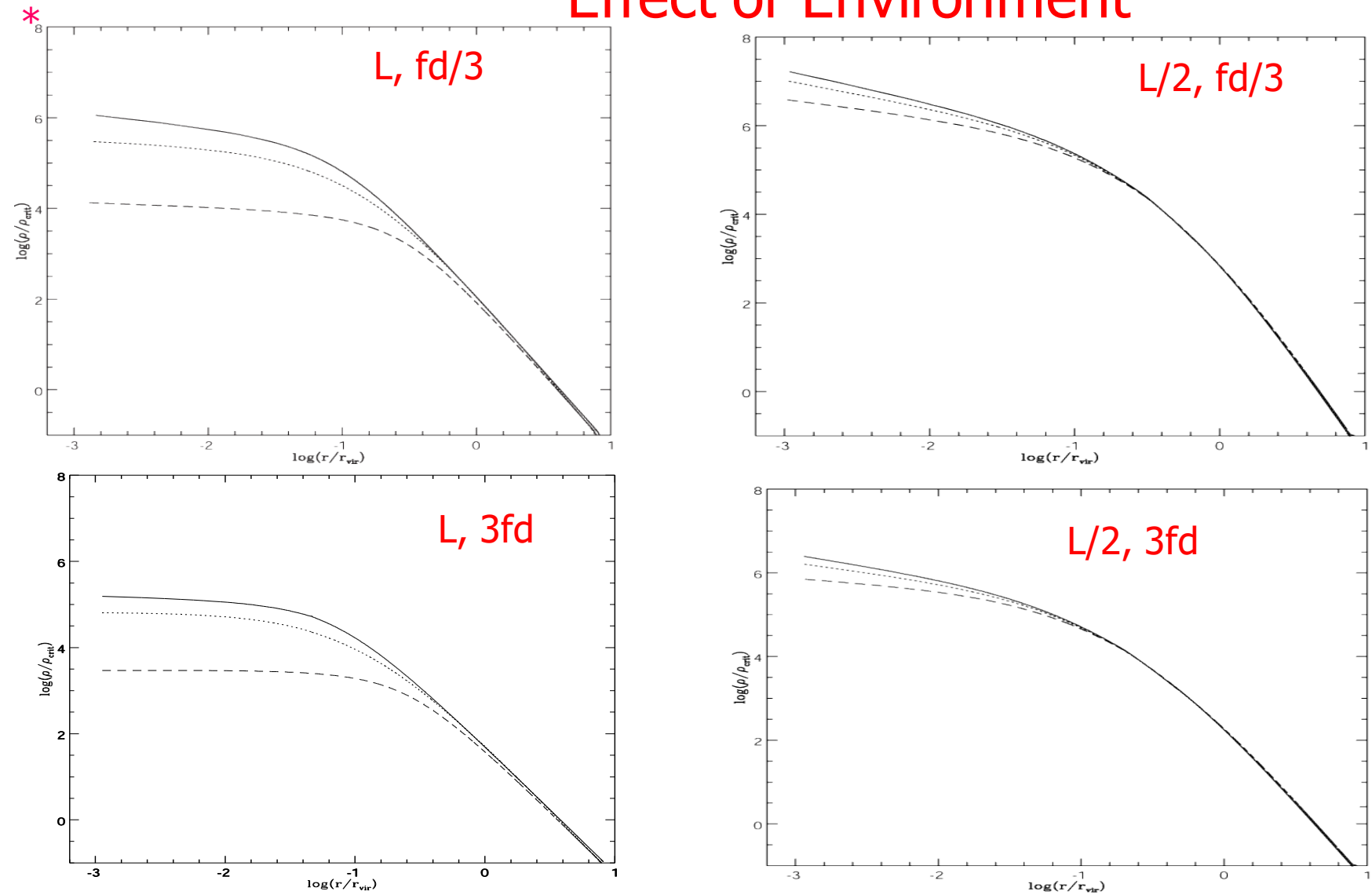
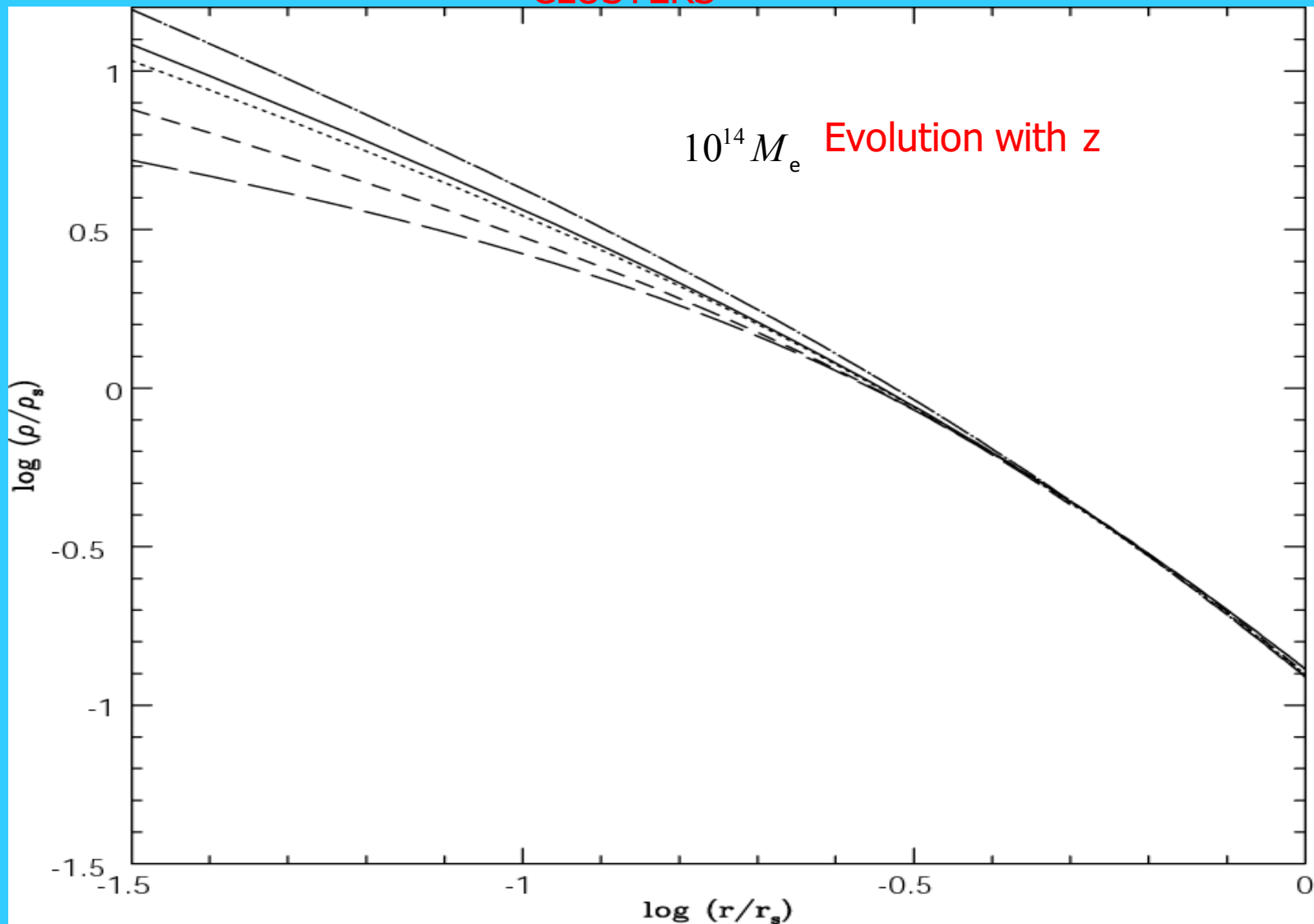
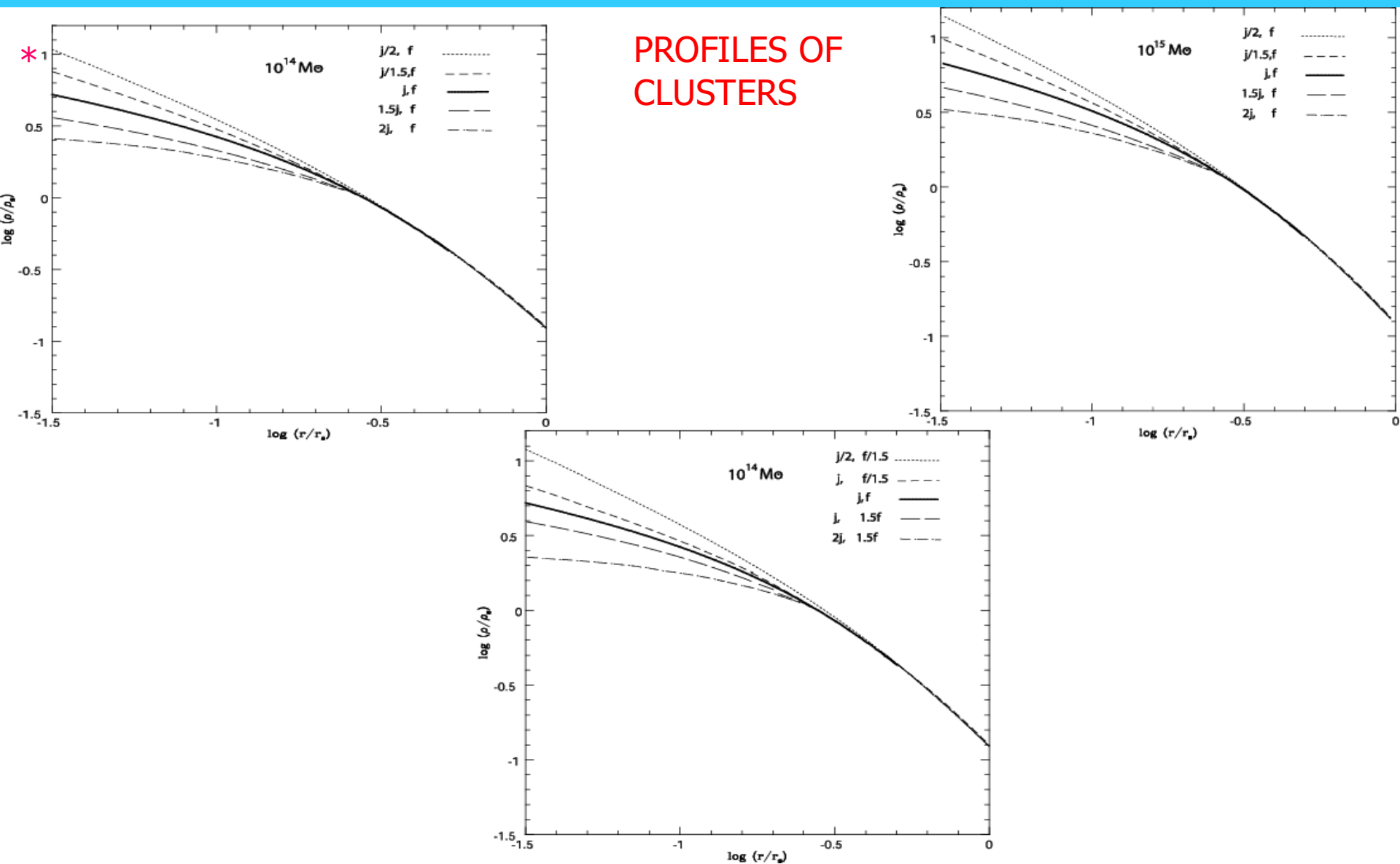


Figure 2 DM halos shape changes with baryon fraction. Same as previous figure, Fig. 1, but in panel (a) we reduced the value of baryonic fraction of Fig. 1a (h, fd) to fd/3, and in panel (b) we reduced the value of baryonic fraction of Fig. 1c to fd/3; in panel (c) we increased the value of baryonic fraction of Fig. 1a (h/2, fd) to 3fd, and in panel (d) we increased the value of baryonic fraction of Fig. 1c to 3fd.



**Figure 5.** Density profile evolution of a  $10^{14} M_{\odot}$  halo. The (uppermost) dot-dashed line represents the total density profile of a  $10^{14} M_{\odot}$  halo at  $z = 0$ . The profile at  $z = 3$ ,  $z = 1.5$ ,  $z = 1$ , and  $z = 0$  is represented by the solid line, dotted-line, short-dashed line, and long-dashed line, respectively.



**Figure 1.** Changes of the density profile with baryonic fraction and random angular momentum  $j$ . Panel (a) refers to density profiles with mass  $10^{14} M_\odot$ , varying only  $j$ . The solid line is characterized by  $F_{B*} = M_b/M_{500} = 0.15$  ( $f_{d*} = 0.88$ ) and  $j = j_*$ . The upper short-dashed line and the dotted line are characterized by  $f_d = f_{d*}, j = j_*/1.5$  and  $f_d = f_{d*}, j = j_*/2$ , respectively. The long-dashed and dot-dashed lines are characterized by  $f_d = f_{d*}, j = j_* \times 1.5$  and  $f_d = f_{d*}, j = j_* \times 2$ , respectively. Panel (b) represents the density profile for haloes of mass  $10^{15} M_\odot$ . Panel (c) shows density profiles for haloes of mass  $10^{14} M_\odot$ , varying both  $j$  and baryonic fraction. The solid, short-dashed and dotted lines are characterized by  $f_d = f_{d*}, j = j_*$ ;  $f_d = f_{d*}/1.5, j = j_*$ ;  $f_d = f_{d*}/1.5, j = j_*/2$ , respectively. The long-dashed and dot-dashed lines are characterized by  $f_d = 1.5 \times f_{d*}, j = j_*$ ;  $f_d = 1.5 \times f_{d*}, j = j_* \times 2$ , respectively.

\*

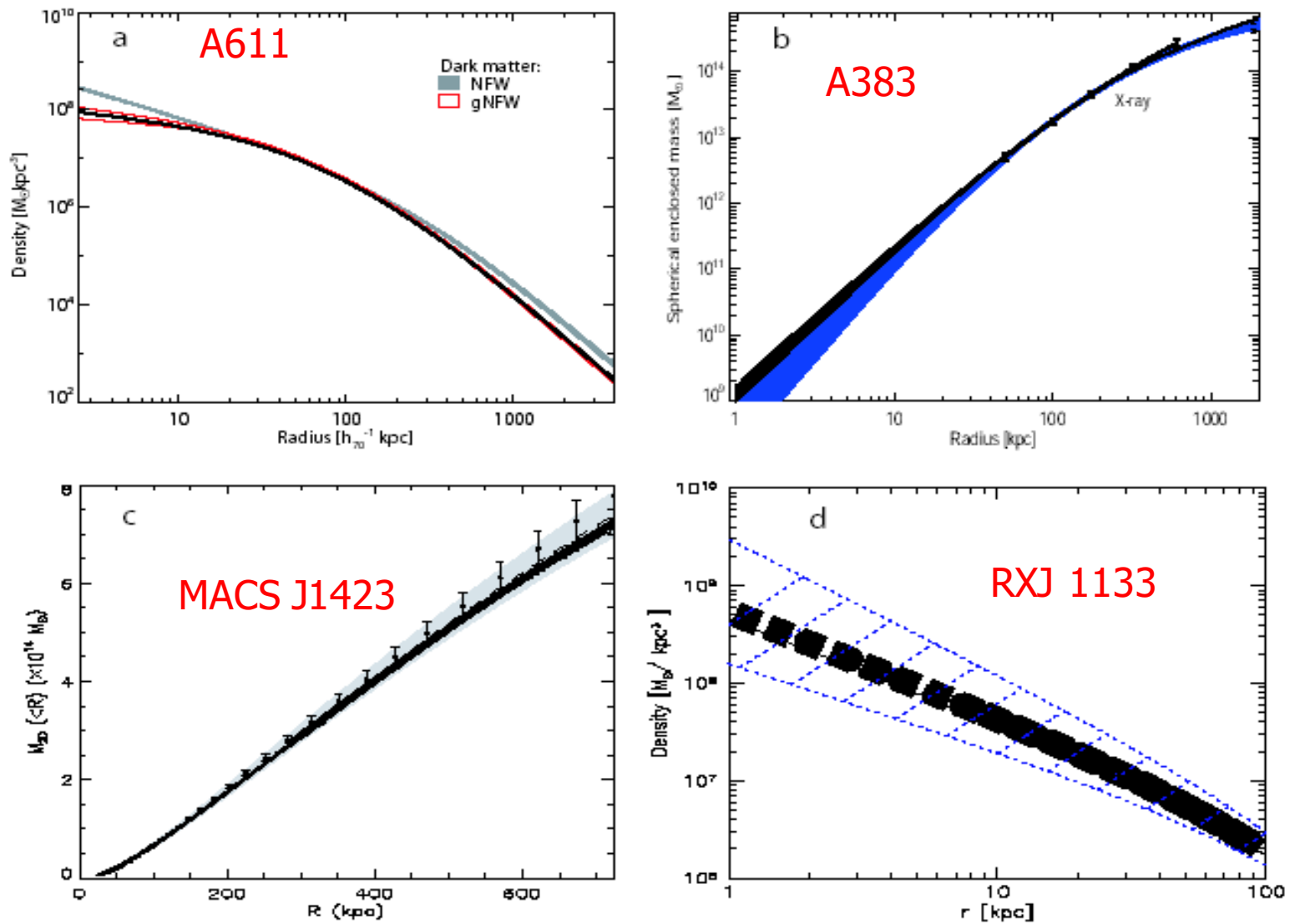


Figure 3. Fig. 3a plots the density profile of A611. The grey solid line is the NFW profile, the red lines bracket the 68% confidence region of the density profile obtained by N09, while the black band is the result of our model. Fig. 3b represents the mass profile of A383. The blue band is the observational result of N11, while the black band the mass distribution obtained with our model. Fig. 3c represents the mass profile of MACS J1423. The azure band with errorbars is the observational result of Morandi, Pedersen & Limousin (2010), while the black band is the result obtained with our model. Fig. 3d represents the density profile of RX J1133. The solid curve and the shaded region are the S04 observational result. The black dashed band is the result of our model. The confidence regions in Fig. 3a-c are  $1 \sigma$  while those in Fig. 3d are  $2 \sigma$ .

# SUMMARY

- Modifying the power spectrum or the DM particles can solve the problem, but it can introduce other problems
- Modifying Gravity: can also solve the problem introducing sometime other problems. Moreover there are not compelling evidences showing knots in GR
- Baryon physics can transform cusps into cores leaving the  $\Lambda$ CDM as it is